U.S. DEPARTMENT OF ENERGY | Energy Efficiency & Renewable Energy

High-Performance Slab-on-Grade Foundation Insulation Retrofits

Louise F. Goldberg and Garrett E. Mosiman
Northern*STAR*

September 2015

Building America
U.S. Department of Energy

Available electronically at http://www.osti.gov/bridge

Available for a processing fee to U.S. Department of Energy
and its contractors, in paper, from:
U.S. Department of Energy
Office of Scientific and Technical Information
P.O. Box 62
Oak Ridge, TN 37831-0062
phone: 865.576.8401
fax: 865.576.5728
email: mailto:reports@adonis.osti.gov

Available for sale to the public, in paper, from:
U.S. Department of Commerce
National Technical Information Service
5285 Port Royal Road
Springfield, VA 22161
phone: 800.553.6847
fax: 703.605.6900
email: orders@ntis.fedworld.gov
online ordering: http://www.ntis.gov/ordering.htm

U.S. DEPARTMENT OF ENERGY | Energy Efficiency & Renewable Energy

High-Performance Slab-on-Grade Foundation Insulation Retrofits

Prepared for:

The National Renewable Energy Laboratory

On behalf of the U.S. Department of Energy's Building America Program

Office of Energy Efficiency and Renewable Energy

15013 Denver West Parkway

Golden, CO 80401

NREL Contract No. DE-AC36-08GO28308

Prepared by:

Louise F. Goldberg and Garrett E. Mosiman

Northern*STAR*

322 Kaufert Laboratory, 2004 Folwell Ave,

St. Paul, MN 55108

NREL Technical Monitor:

Prepared under Subcontract No. KNDJ-0-40340-05

September 2015

The work presented in this report does not represent performance of any product relative to regulated minimum efficiency requirements.

The laboratory and/or field sites used for this work are not certified rating test facilities. The conditions and methods under which products were characterized for this work differ from standard rating conditions, as described.

Because the methods and conditions differ, the reported results are not comparable to rated product performance and should only be used to estimate performance under the measured conditions.

Contents

List of Figures

Unless otherwise noted, all figures were created by the NorthernSTAR team.

List of Tables

Unless otherwise noted, all tables were created by the NorthernSTAR team.

Definitions

BCVTB	Building Controls Virtual Test Bed
BEB	BUFETS-B/EnergyPlus/BCVTB
BEopt™	Building Energy Optimization
BUFETS-B	BUilding Foundation Energy Transport Simulation-BCVTB
EIA	Energy Information Administration
ELA	Effective Leakage Area
Eplus	EnergyPlus
FPSF	Frost-Protected Shallow Foundation
FTF	Foundation Test Facility
IECC	International Energy Conservation Code
M-H	Mixed-Humid Climate
OSB	Oriented Strand Board
PPU	Poured Polyurethane
RH	Relative Humidity
SIP	Structural Insulated Panel
SOG	Slab-on-Grade
USGS	U.S. Geological Survey
VC/C	Very Cold/Cold Climate
XPS	Extruded Polystyrene

Executive Summary

The U.S. Department of Energy's Building America research team Northern*STAR* completed a project to more accurately assess slab-on-grade (SOG) foundation insulation energy savings than has been traditionally possible. Advances in whole-building energy simulation have enabled this research, including three-dimensional foundation modeling integration at each time step and an experimental measurement of the site energy savings of SOG foundation insulation.

The objectives of this project were to:

- Calculate the possible site and source energy savings for optimal insulation retrofits for SOG foundations in U.S. climate zones 4–7 for single- and multifamily homes.
- Determine how these energy savings are dependent in real-world houses on the critical <slab heat flow>/<site energy consumption> ratio (β).

The BUilding Foundation Energy Transport Simulation-B/EnergyPlus/BCVTB model was compared against measured site energy data that were generated by vertical and wing stem insulation installed on a frost-protected shallow foundation. The simulated and experimental site energy results agreed within 7% –3.2%/+3.4%. Lower errors were not possible because of the difference between the experiment and simulation slab boundary conditions. In comparison, the repeatability of the experimental results over three heating seasons with different mean temperatures and cumulative snow depths was 0.7%. The principal experimental error was the potential for different air leakage rates in the test and reference modules, which were estimated by simulation to be ±3%. Several physically reasonable causes for the discrepancy in the simulation were identified; principally, the inability of EnergyPlus to accurately model the fairly complex slab surface heat transfer in the experimental test buildings. The effect of the error in the simulated site energy results was to underestimate the site energy savings that are possible from SOG insulation.

Ten SOG insulation strategies were evaluated on a test building with a high value of β = 0.527 in a zone 6 climate (Minneapolis, Minnesota). More than half the enclosure heat loss was through the slab. This is not representative of typical retrofit construction, but it provides the high signal-to-noise ratio that is necessary to distinguish clearly between the insulation strategies evaluated. The optimum insulation strategy in terms of energy savings and cost-effectiveness consisted of two components:

- R-20 extruded polystyrene insulation above grade.
- R-20 insulation at grade tapering to R-10 insulation at half the below-grade wall height. This configuration comprised an outer layer of R-10 XPS and an inner layer of poured polyurethane. The lower half of the stem wall was uninsulated.

The optimum insulation strategy yielded site energy savings of 36.3% at an installed cost of $16.15 per linear foot. For comparison, the SOG foundation insulation required by the 2012 International Energy Conservation Code yielded site energy savings of 27.6% at a cost of $17.94 per linear foot.

The optimum insulation strategy identified for zone 6 was applied to single- and multifamily residential buildings in climate zones 4–7, because the research plan did not permit the evaluation of climate-specific optimized SOG insulation retrofit strategies. Although this assumption is reasonable for zone 7 and likely satisfactory for zone 5, it may not be true or cost-effective for zone 4. Therefore, alternative strategies were evaluated for zone 4. These buildings were designed using the National Renewable Energy Laboratory's Building Energy Optimization software and complied with (1) the standard Building America protocols for occupant lifestyle effects and (2) the B10 benchmark enclosure specification with some energy performance improvements. For single-family homes, the site energy savings ranged from 3.1% in zone 4 to 5% in zone 7. The principal reason for the much lower savings relative to the zone 6 evaluation test building was the large difference in the value of β, 0.527 for the test building compared with 0.186 (zone 4) and 0.141 (zone 7) for the retrofit building. The site energy savings are a nonlinear function of β, so small changes in β produce larger changes in the site energy savings. These energy savings generated simple paybacks of 17.9 and 45.4 years in zones 4 and 7, respectively. In the case of a multifamily home that comprises two center and two end units, the site energy savings ranged from 1.4% in zone 4 to 2.6% in zone 7 and yielded simple paybacks of 18.5 and 45.6 years for zones 4 and 7, respectively. In source energy terms the savings were lower; 2.4%–3.9% for single-family homes and 1%–1.8% for multifamily homes.

An approximate design equation was developed to assess the likely energy savings performance of SOG foundation insulation. Applying this equation suggests that 10% site energy savings from optimized SOG foundation insulation becomes possible only when the combined above-grade enclosure and occupant lifestyle energy consumption fraction of the site energy is reduced to 62% or lower for zones 5–7 and 25% or lower for zone 4. Thus, to achieve high levels of whole-building cost-effective retrofit site energy savings (>25%), SOG foundation insulation has a considerably lower priority than other measures in zones 5–7. In zone 4, it is likely never appropriate, because achieving a combined enclosure and occupant lifestyle energy load of 25% or lower is exceedingly difficult in practice.

In summary, significant reductions in slab heat flow of 15%–31% can be achieved from optimized SOG foundation insulation. However, when combined with the small values of β in target retrofit real-world houses (0.127–0.141 and 0.073–0.112 for single- and multifamily homes, respectively), the slab heat flow reductions result in modest site energy savings of 5% or lower, which are not cost-effective. (Simple paybacks are mostly longer than 40 years, except in zone 4, which has paybacks longer than 17 years.)

Other benefits of SOG foundation insulation result from the increase in the slab surface temperatures. These benefits include increased occupant comfort from reduced radiant heat exchange with the slab and a potential decrease in slab surface condensation, particularly around the slab perimeter.

1 Problem Statement

1.1 Introduction

Slab-on-grade (SOG) foundation insulation retrofits have perhaps received less attention than full basement and crawl space insulation retrofits, because the latter are easier to accomplish—they can be installed on the interior of the foundation. Recent soil excavation methodologies, such as hydro-vacuum excavation, may significantly reduce installation costs. The thermal performance of SOG foundation insulation was last evaluated comprehensively in the late 1980s using obsolete simulation methodologies (Labs et al. 1988). The results tended to yield overestimates of the heating season energy savings that may accrue from insulating SOG foundations and whole-year negative energy savings. That is, the cooling season increase in energy consumption that results from SOG insulation exceeded the heating season savings. More accurate simulation methodologies have since become available, and empirical data have been developed that enable these methodologies to be compared with experimental performance in terms of seasonal energy consumption.

The U.S. Department of Energy's Building America research team Northern*STAR* aimed to use improved simulation methodologies and modern installation techniques to develop a cost-effective SOG retrofit insulation methodology that optimizes both thermal performance and installation cost. This methodology offers the potential of maximizing the energy savings that are achievable from insulating SOG foundations and thus maximizes the potential of SOG retrofit foundations to contribute to achieving the Building America goal of 50% energy savings relative to 2009 International Energy Conservation Code (IECC) levels.

1.2 Background

Research conducted at the University of Minnesota's Foundation Test Facility (FTF) demonstrated that R-10 vertical and wing insulation applied to a shallow SOG foundation yielded 13.6% site energy savings for the specific experimental configuration tested in zone 6 compared with an uninsulated stem wall foundation with a frost footing (Goldberg 2014). Work was conducted for the (then) National Association of Home Builders that led to frost-protected shallow foundations (FPSFs) being included in the IECC (HUD 1994). Techniques for including three-dimensional earth contact thermal analysis into Building Energy Optimization (BEopt™)/EnergyPlus were demonstrated by Goldberg and Steigauff (2013). Modern techniques for excavating soil around a building foundation (such as hydro-vacuum excavation) have been successfully demonstrated (Schirber et al. 2014). This project is intended to combine effective insulation strategies (such as those developed for FPSFs) with modern soil excavation techniques to design an optimized SOG foundation insulation retrofit approach. This approach theoretically would yield the highest cost-effectiveness possible for SOG foundation insulation.

1.3 Relevance to Building America's Goals

Developing cost-effective SOG foundation retrofit insulation systems is listed in the document "Building America Technical Innovations Leading to 50% Savings" as being on the critical path (section E5). This measure also meets the criteria of the U.S. Department of Energy FY 2012 Statement of Need in Sections 1.0 (High-Impact System Innovations) and 2.0 (Risk Reduction and Minimization). If the already demonstrated 13.6% site energy savings can be achieved in existing real-world SOG homes, this would yield more than 25% of the desired 50% target. An improvement in this performance is feasible simply by increasing the insulation and optimizing its distribution around the slab perimeter. Such insulation systems have to be designed with care to avoid frost heave structural failure and to avoid compromising the integrity of the insulation as a consequence of soil/insulation adfreeze and other effects. Modern soil excavation techniques may deliver the experimentally demonstrated or higher energy savings at significantly lower installation costs. Achieving these results will produce a SOG insulation retrofit measure guideline for installing an optimum system in climate zones 4–7 (cold and mixed climates). The potential extent of deployment of such a system has been estimated from the 2011 American Housing Survey for the United States (HUD and Commerce 2013) as follows:

- The total number of housing units on a concrete slab is reported as 30.43 million (Table C-01-AH).
- The total number of homes in all regions is reported as 132.419 million.
- The number of homes in zones 4–7 (approximated as the aggregate of the New England, Midwest, and Mountain West regions) is reported as 45.612 million (Table C-00-AH).
- Assuming the SOG home fraction is uniform across the included regions, the potential retrofit market is about 10.48 million homes.

1.4 Objectives

The primary objective was to calculate the site and source energy savings possible for an optimal SOG foundation insulation retrofit in climate zone 6 and then apply this retrofit to U.S. climate zones 4–7 for single- and multifamily homes. These savings then could be used to determine the cost-effectiveness of such an optimal insulation strategy for each building type in each climate zone.

The secondary objective was to determine the magnitudes of site and source energy savings that are possible for real-world SOG insulation retrofits in which the <slab heat flow>/<site energy>ratio is generally less than 20% based on experiment (Goldberg et al. 1994). Previous research for full basement insulation retrofits in real-world homes (Goldberg and Steigauf 2013) has engendered considerable skepticism about heating season site energy savings reported by Labs et al. (1988). For example, these authors report heating season savings of about 10%–14% in zone 6. The actual savings likely are somewhat smaller.

The following research questions were also addressed:

1. Can the experimentally measured site energy savings of a SOG foundation insulation in a cold climate be replicated by the Building Controls Virtual Test Bed (BCVTB) EnergyPlus/BCVTB (BEB) simulation model?
2. What is the energy performance and installation cost of a range of technically feasible SOG foundation insulation retrofit systems in climate zone 6?
3. Can the experimentally measured site energy savings in zone 6 be met or exceeded in cold and intermediate climates by cost-effective SOG insulation strategies such as those developed for FPSFs?
4. What is the optimum SOG insulation retrofit strategy in zone 6 in terms of absolute energy savings and energy savings/retrofit cost/unit length of perimeter?

5. What is the energy performance of the selected optimum zone 6 SOG insulation retrofit strategy in four cities that span climate zones 4 through 7 for single- and multifamily homes?
6. What is the installation cost of the optimum SOG insulation retrofit strategy in the four cities evaluated and the resultant cost-effectiveness of the retrofit measure?

2 Simulation Methodology

The simulation methodology deployed takes an additional evolutionary step over that used in two previous Building America projects. In the earlier work (Goldberg and Steigauf 2013; Huelman et al. 2015), the BUFETS revision C (BUilding Foundation and Energy Transport Simulation) program was combined with the U.S. Department of Energy's EnergyPlus revision 6.0.0 whole-building energy simulation program to enable three-dimensional foundation heat transfer simulation.[1] In this methodology, BUFETS and EnergyPlus were decoupled so BUFETS was executed first to generate the foundation enclosure heat fluxes that were subsequently imported into EnergyPlus, which was executed next.

For this mechanism to be effective, the interior foundation enclosure boundary conditions must be identical in BUFETS and EnergyPlus at every time step. This is reasonable when a basement that is conditioned to a known temperature set point schedule is being considered. However, most conditioned basements have uncontrolled temperatures because thermal space conditioning is supplied only when the thermostat, which is typically located in an above-grade portion of the building, calls for it. Therefore, the basement temperatures are transient and cannot be determined with any accuracy *a-priori*. Ideally, this requires an iterative execution of BUFETS and EnergyPlus until the basement temperatures converge. In view of the extremely long execution time for BUFETS to simulate a full year (approximately 30 hours for 126,000 control volumes), such an iterative approach was not tractable for the large number of cases simulated. Hence, for a once-through methodology to be numerically stable, the BUFETS foundation interior air temperatures must be equal to or higher than the EnergyPlus foundation interior air temperatures at every time step. In this case, the model is stable and the simulated heat fluxes through the interior foundation surfaces will be in error and nonlinearly proportionate to the difference between the temperature profiles. When the EnergyPlus floating temperature boundary condition temperatures exceed those used in BUFETS, the coupling mechanism becomes unstable and the combined simulation yields physically invalid results.

Just before the simulation part of this project started (but after the test plan was submitted) a new version of BUFETS, called BUFETS-B (revision A) was made available by its developer for use in the project. The -B appendage denotes compatibility with the Building Controls Virtual Test Bed (BCVTB) platform developed by Lawrence Berkeley National Laboratory.[2] This platform allows various commonly used independent programs such as EnergyPlus, TRNSYS, MATLAB, and Simulink to be linked together so they can exchange data at every simulation time step. EnergyPlus and BUFETS-B can now be linked together so they operate in unison as a combined simulation. Specifically, at every simulation time step, EnergyPlus provides the interior foundation enclosure surface boundary temperatures to BUFETS-B, and BUFETS-B provides the resulting foundation interior surface heat flows to EnergyPlus.[3] In effect, this allows BUFETS-B to be run as a subroutine of EnergyPlus. This methodology represents the ideal theoretical construct and yields an unconditionally stable combined simulation program in which

[1] BUFETS is a proprietary, noncommercial software program developed by Lofrango Engineering, Minneapolis, Minnesota. A full description of BUFETS and the original BUFETS/EnergyPlus coupling methodology is provided in Goldberg and Steigauf (2011).
[2] http://simulationresearch.lbl.gov/bcvtb.
[3] The details of the coupling mechanism in EnergyPlus are described in Goldberg and Steigauf (2011).

EnergyPlus can directly thermally simulate the ground around the foundation enclosure and the enclosure components (walls, slab, insulation, etc.) in three dimensions. It also allows the full set of interior boundary heat flows (convection, direct solar gain, and infrared radiation) to be included in the BUFETS-B simulation. Thus the BEB software was used in this project in view of its significantly improved capability relative to the original BUFETS/EnergyPlus combination used previously.

The salient features of BUFETS-B are:

- Nonlinear material properties as arbitrary functions of temperature and moisture content
- Three-dimensional geometry
- Arbitrary, time-dependent boundary conditions
- Boolean geometry specification and mesh generator
- Based on a rigorous implementation of the generalized transport theorem of continuum mechanics (Slattery, 1981)
- Inclusion of fully discontinuous phase change physics with frost-front tracking
- Stable proprietary solver (enables multiyear real time simulation of large discrete volume meshes [more than 100,000 volumes])
- Graphical animation outputs
- Arbitrary coupling of data outputs (fluxes, temperatures, U-values)
- 8,760 hours simulated per year with an arbitrary time step size (typically 1 hour to comply with standard Typical Meteorological Year weather data)
- Snow depth model, including the effect of snow compaction in calculating the equivalent thermal resistance
- Interface to the BCVTB platform developed by Lawrence Berkeley National Laboratory.

BUFETS-B also has the following limitations:

- No inclusion of any gaseous (air, water vapor) transport. Hollow masonry block walls cannot be accurately modeled, especially when the cores have a buoyant cavity flow. This also applies to porous interior insulation such as fiberglass batts.
- No inclusion of any bulk water transport. The soil moisture content field is entered as a simulation parameter and held constant.

The overall BEB (including EnergyPlus version 8.1) coupled simulation program methodology is described in the flowchart of Figure 1. A three-dimensional BUFETS-B model of the SOG foundation is prepared based on the dimensions of the BEopt EnergyPlus whole-building model. Generally, axes of symmetry in the BEopt model are used to minimize the BUFETS-B simulation domain (see Figure 8 for an example). The model is input to a mesh generator that prepares all the geometry input files necessary to execute BUFETS-B. The BUFETS-B boundary and initial condition input files also are prepared. The foundation slab geometry in the EnergyPlus input file is modified to be compliant with the BUFETS-B foundation model. In this project, the slab surface was modeled using three zones as follows (see Figure 8):

- A 24-in.-wide edge zone around the perimeter
- 44-in.-long by 24 in. wide corner zones in each corner
- A center zone for the balance of the slab.

Finally, the BUFETS-B and BCVTB coupling fields are added to the EnergyPlus model. The overall combined model is then executed for the chosen time period (in this project, 8,760 hours) with time increments of 15 minutes to permit adequate capture of thermal transients (Tabares-Velasco 2013).

In this project, each simulation was run for 2 years. The ground temperature field around the foundation was initialized during the first year; the simulation results were generated during the second year. These results included the standard BEopt output results as well as additional results files for BUFETS-B and EnergyPlus that were used to prepare graphs of the slab surface temperatures and to verify that the slab surface heat flows output by BUFETS were the same as those input to EnergyPlus.

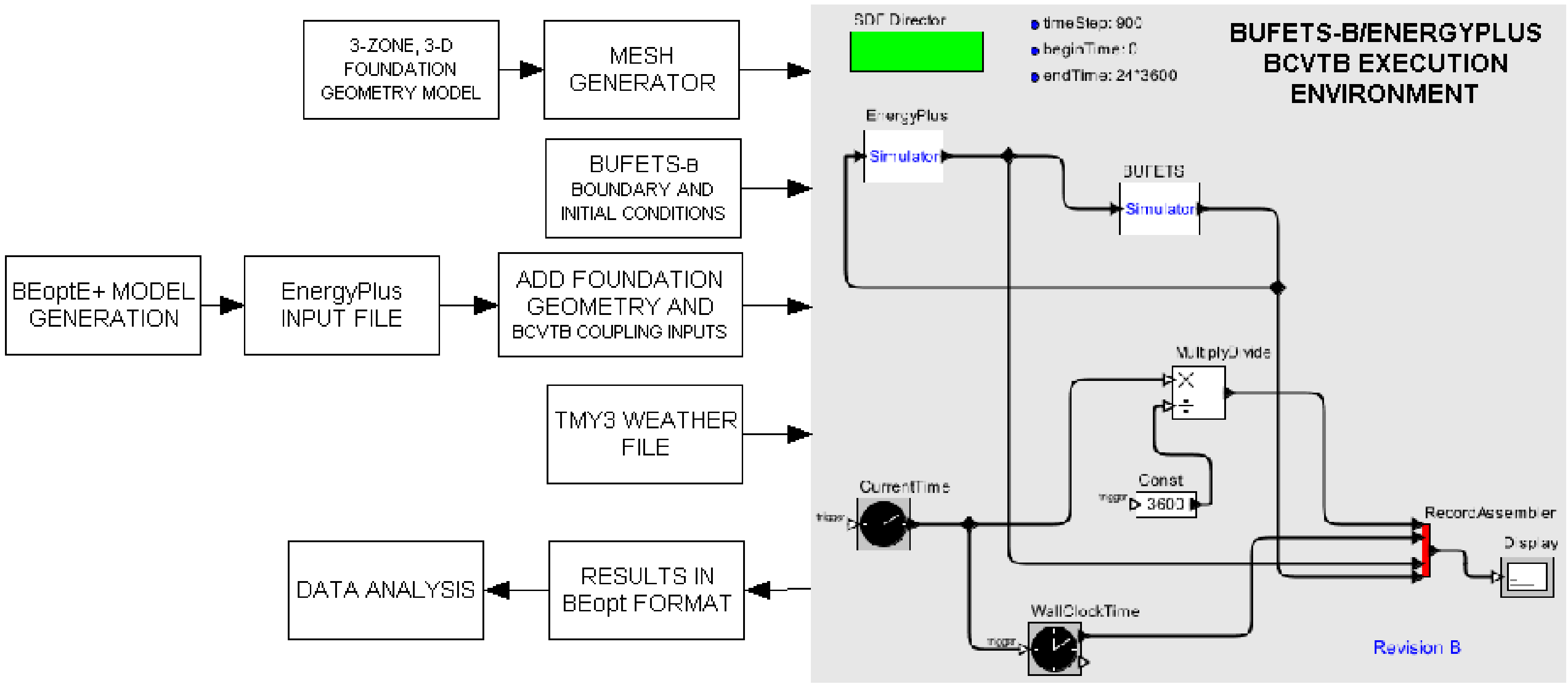

Figure 1. BUFETS-B/EnergyPlus simulation program schematic

3 Comparison of the Simulation Methodology Energy Predictions with Experimental Data

A recent search of the technical literature from 1884 to the present did not yield a single publication that reported any experimental data for the heat transfer through the whole slab surface together with the overall building energy consumption of buildings with SOG foundations, the core data on which the project is based. In contrast, several publications report either analytical or simulation results (for example, Khaled et al. 2012; Chuangchid and Krarti 2001). Comparisons of experimental and simulation SOG foundation temperatures also exist (for example, Adjali et al. 2000), but these omit area-integrated slab surface heat flows. Emery et al. (2007) report measured basement slab point heat fluxes, but area-integrated slab surface heat flows are not reported. Whole-building experimental data are particularly important for assessing the energy performance predictions from the BEB model in which the modeled interactions between the foundation and the building also need to be assessed, not just the foundation simulation alone. For example, analytical validation methods (such as those given in Neymark and Judkoff 2008) that assess only the accuracy of a linear foundation heat transfer simulation are not sufficient[4]. Hence, the only whole slab SOG experimental data known by the authors is reported in an unpublished University of Minnesota research report (Goldberg et al. 1994).[5] Thus these data are used here to compare the energy performance predictions of the BEB simulation methodology that were applied to SOG foundations to available experimental data.

The data were collected during the heating seasons of 1991–1992, 1992–1993 and 1993–1994 at the University of Minnesota's FTF.[6] The Energy Systems Design Program building foundations website includes the complete description of the experiment and the methodology used to measure the slab heat flow.[7] The experiment comprised two 20 × 20 ft square test modules (Figure 2). The reference module was an uninsulated SOG; the stem wall extended 42 in. below grade (6 in. topsoil and 36 in. imported sand fill), and the test module had an insulated shallow frost-protected stem wall that extended just 16 in. below grade. Neither module had a conventional spread footing (the stem wall rested directly on the soil) to simplify the heat transfer through the foundation wall. The test module insulation comprised R-10 extruded polystyrene (XPS) full-depth vertical insulation with 24-in.-wide R-10 XPS wing insulation at both the corners and the center of the wall. The above-grade structures were fabricated entirely from large structural insulated panels (SIPs) that comprised a sandwich of 3.5 in. expanded polystyrene insulation between two layers of 0.5-in. oriented strand board (OSB) sheathing. The sheathing was painted on the exterior and unfinished on the interior. Because only seven SIPs were used to construct the modules (four for the walls and three for the roof), the number of joints and the infiltration effective leakage area (ELA) were minimized.

The apparatus shown in Figure 4 and Figure 5 was used to measure the heat flow through the slab. The physical layout depicted in Figure 3 and Figure 4 shows that a flow-through cavity was

[4] BUFETS has been successfully tested against the IEA BESTEST analytic solution (Case GC10a) (Neymark and Judkoff 2008). The test results are included in an article that has been accepted for publication in the Journal of Green Building (planned for the January, 2016 issue).

[5] Full basement data from this research report are used in Adjali et al. 1998.

[6] http://www.buildingfoundation.umn.edu/ftf.htm

[7] http://www.buildingfoundation.umn.edu/description.htm

created above the slab that was guarded around its outer perimeter by a rim duct through which heated interior air was circulated. The slab and room cavities were separated by a 6.5-in. SIP with a nominal R_{US} value greater than 26. The slab surface was split into 12 radial flow sectors with separate induction fans in each sector. As shown in Figure 5, transducers were installed to measure the total flow rate through all the sectors, the inlet and outlet temperatures of each sector, the air temperatures in the airstream at two locations, and the temperatures on the room side of the SIP just above the slab cavity air temperatures. These measurements allowed the total enthalpy drop across the radial flow paths and the heat loss through the SIP to be calculated. The difference between these measurements yielded the net heat flow through the slab. The data acquisition system also recorded the energy flow in increments of 10 Wh on a counter in each module for manual recording purposes.

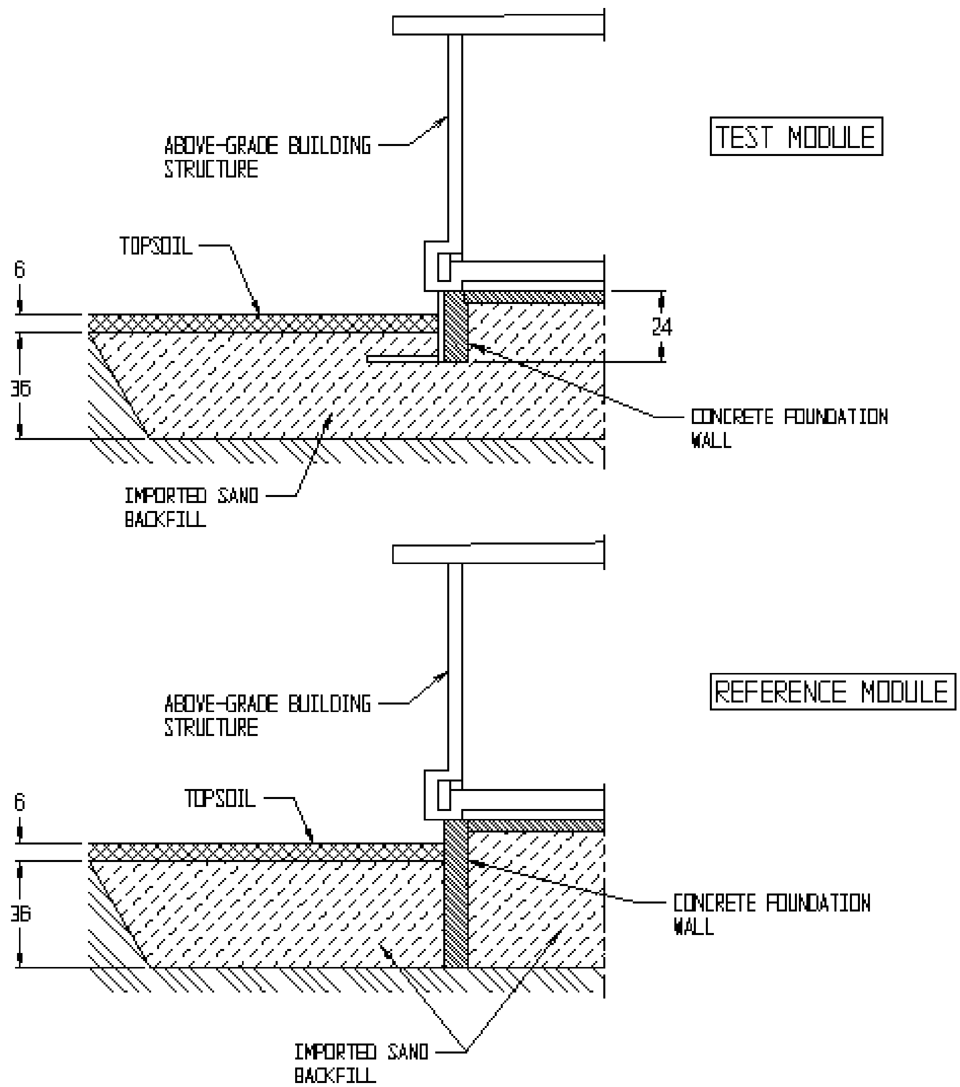

Figure 2. SOG test module physical configuration

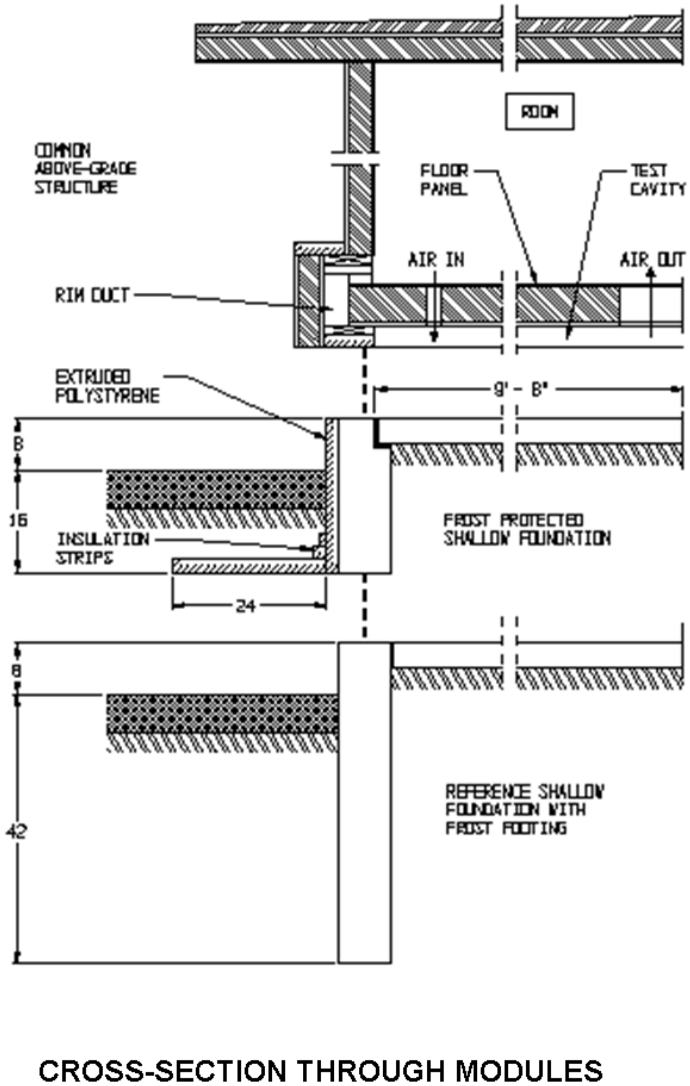

Figure 3. Cross-sectional view of the slab heat flow monitoring layout

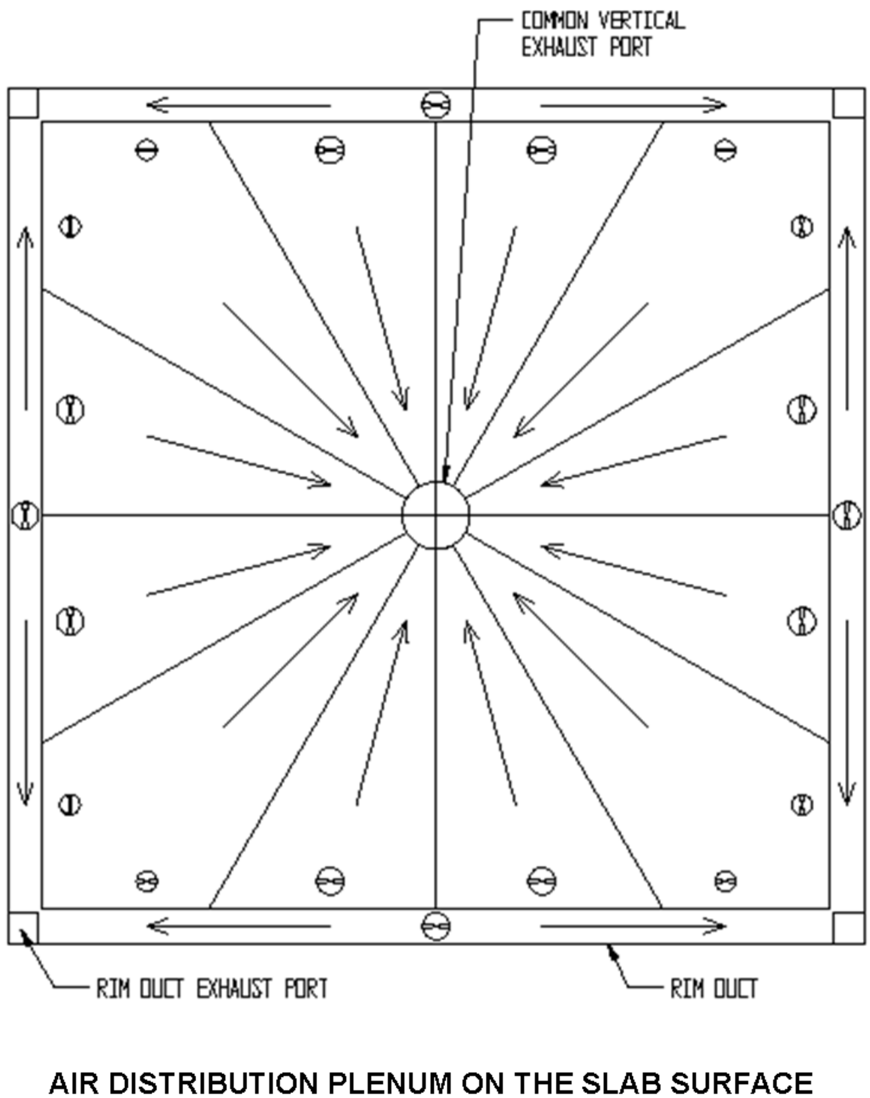

Figure 4. Plan view of the slab heat flow monitoring physical layout

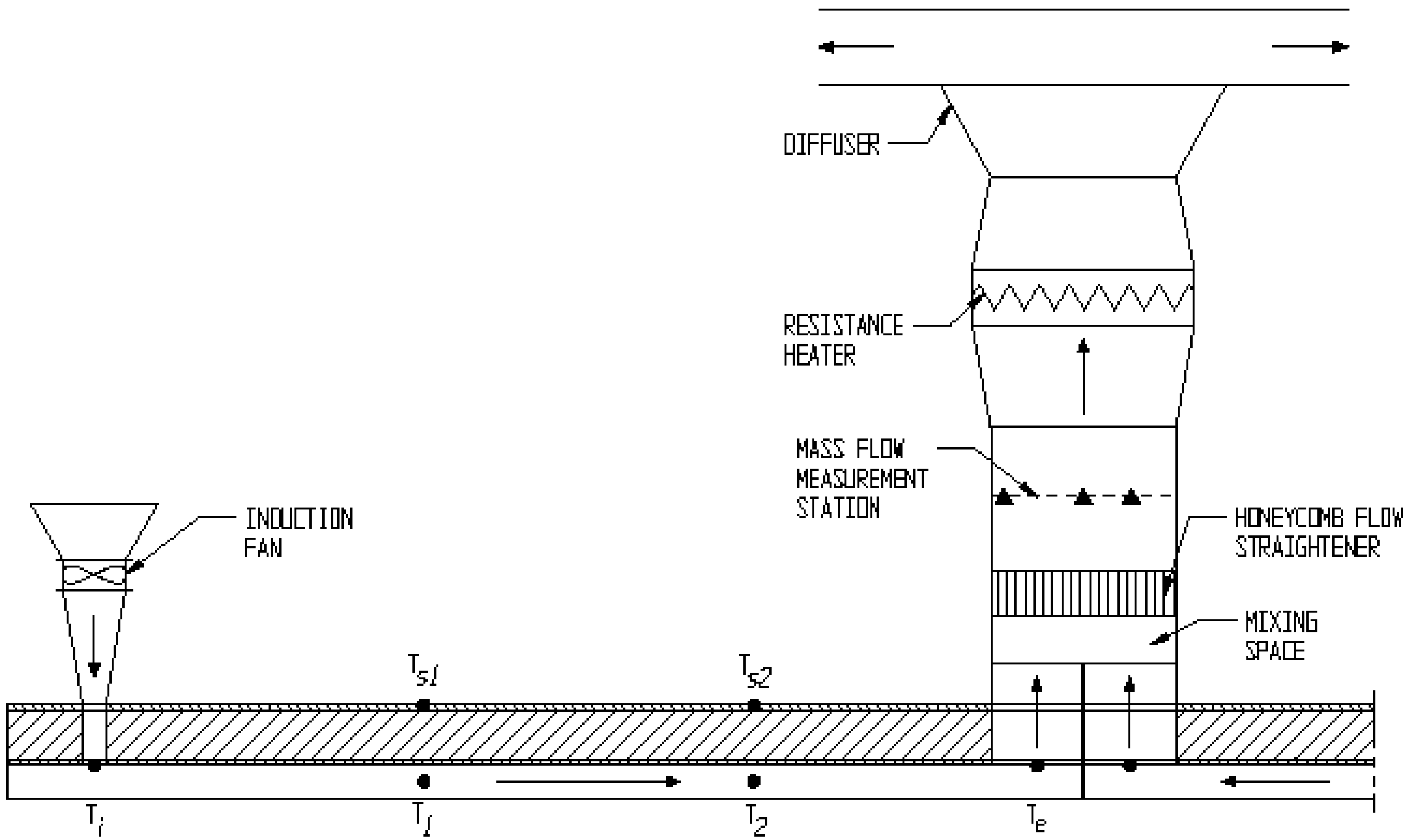

Figure 5. Slab heat flow monitoring instrumentation

The modules were electrically heated, and the total energy consumed by each module was measured by a rotating disc watt-hour meter that provided a direct measurement of the site energy consumption.

A large quantity of experimental data was collected for the two modules, including transient measurements of the slab and stem wall temperatures and the data from the slab heat flow monitoring systems. However, most unfortunately, all these data were lost when the Underground Space Center at the University of Minnesota was permanently closed in 1995.[8] Only the manual watt-hour meter and slab energy flow readings collected each week during the experiment remain. These data are given in Table 1. The test modules were heated for the full 1991–1992 and 1992–1993 seasons but only through the beginning of January in 1993–1994 when the heating plant was turned off to conduct a frost penetration test. This test measured the time for the frost to penetrate beneath the footings on the FPSF test module without any interior heat. The slab heat flow monitoring system was not operational during the 1993–1994 heating season experiment.

Table 1. SOG Module Experimental Data

Test Heating Season	Duration	Reference Module (uninsulated)		Test Module (insulated)	
		Site Energy Consumption (kWh)	Slab Heat Flow (kWh)	Site Energy Consumption (kWh)	Slab Heat Flow (kWh)
1991–1992	12/11/1991-14h10 to 4/30/1992-13h32	3,607	715.22	3,092	445.38
1992–1993	11/24/1992-15h56 to 4/30/1993-8h39	4,377	787.06	3,778	447.36
1993–1994	10/29/93-14h57 to 1/3/94-12h03	1,836	No measurement	1,596	No measurement

The theoretical basis of the experiment was to use the reference module for data normalization so differences in transient weather and soil moisture conditions could be factored out of the results and compared over multiple seasons. To this end, both test and reference modules were engineered to be as close to identical as possible including the imported sand backfill so that, in theory, the only significant difference between the modules was the foundation configuration. Thus, a normalized comparison of the data strictly demonstrates the effect of the insulated frost-protected footing in the test module on the module energy performance. A further benefit of the experimental design is that it also allows the normalized data to be used for simulation testing, provided these data are also normalized and the only difference between the reference and test simulation models is in the foundation configuration. That is, the weather, the surrounding soil,

[8] This is the reason the data were never published.

and the soil moisture content used in the simulation can all be different from those in the experiment as long as they are the same in all the simulations. This methodology also requires the simulation to replicate the enclosure heat transfer physics of the experimental modules as accurately as possible.

However, whether the theoretical similarity between the experimental above-grade structures was achieved in practice is unknown, because all the qualification data were lost. In particular, whether the modules had the same measured infiltration rate (which is the most likely as-built difference) is unknown. The effect of different infiltration rates in the two modules was investigated parametrically.

Table 2 shows the relevant normalized experimental results. The site energy consumption ratio γ over the three heating seasons had a value of 0.863 ±0.006, which yielded a maximum deviation from the average of 0.7%. Further, because σ and β (defined in Table 2) differed from 1991–1992 to 1992–1993, these data cannot be considered steady-state. This is also evident from Table 1 in which the 1992–1993 site energy measurements were larger than those of 1991–1992 for both modules. This indicates colder heating season ambient temperatures. However, from Table 2, the slab energy flow fractions β_R and β_T were lower in 1992–1993 than those in 1991–1992. This indicates that despite the colder ambient temperatures in 1992–1993, the snow around the test modules was deeper. These inferences were confirmed by a review of the 1991, 1992, and 1993 local climatological data summaries for the Minneapolis-St. Paul airport weather station downloaded from the National Climatic Data Center.[9] The climate conditions in 1991–1992 and 1992–1993 were quite different: the 1993–1994 heating season was less than half the length of the previous 2 years, and γ still deviated by less than 1%.

Table 2. Normalized SOG Module Experimental Data

Test Heating Season	Site Energy Consumption Ratio (γ) (Test/Reference)	Slab Heat Flow Ratio (σ) (Test/Reference)	Reference Module Slab Energy Fraction (β_R) (Slab/Site)	Test Module Slab Energy Fraction (β_T) (Slab/Site)
1991–1992	0.857	0.623	0.198	0.144
1992–1993	0.863	0.568	0.180	0.118
1993–1994	0.869	N/A	N/A	N/A

It was thus decided to use the 1992–1993 heating season as the simulation basis because it corresponded with the mean value of γ. Figure 6 and Figure 7 show the simulation test module configurations. The geometry of the foundations in both models was made identical to that of the experimental modules, including the slab edge expansion joints and the two guard insulation blocks at the junction of the vertical and wing insulation in the test module (Figure 7). However, the superstructure was simplified in the following ways:

- The slab heat flow measurement apparatus was removed because EnergyPlus cannot replicate the heat transfer conditions above the slab. Also, all the relevant data, such as the measured system flow rates and temperatures, have been lost. A configuration with a

[9] http://www.ncdc.noaa.gov/IPS/lcd/lcd.html.

separate cavity zone above the slab with an estimated airflow rate of 1,882 cfm[10] between the slab cavity and the room was simulated for comparison with the single-zone convective coupling approach shown in Figure 6 and Figure 7. Numerically, the single-zone and dual-zone approach yielded site energy (watt-hour meter reading) results within 3% of each other for a January test period. Thus, the single-zone approach was adopted for simplicity and consistency between the test and reference modules.

- The door was removed.
- The modules were assumed to be fairly airtight with an ELA of 3 cm^2, because no infiltration data for the experimental test modules could be found.

Other than these modifications, the simulation and experimental modules had the same geometry and materials. Table 3 provides the aggregated set of material properties that were used for all the simulations described in this report. The soil thermal properties were based on the skeleton properties shown and the properties of air and water in proportions that were dependent on the porosity and the saturation ratio. The soil thermal conductivity was calculated using Johansen's method (Johansen 1975) as a function of temperature, porosity, and saturation ratio.

Table 3. Simulation Material Properties

Material	Skeleton Density (kg/m^3)	Skeleton Heat Capacity (J/kg/K)	Porosity	Thermal Conductivity (W/m.K)	Density (kg/m^3)	Heat Capacity (J/kg/K)
Oak Ridge National Laboratory Sand	2,648.51	850.04	0.404	variable (Johansen's method)		
Oak Ridge National Laboratory Silt Loam	2,605.91	850.05	0.448	variable (Johansen's method)		
XPS	N/A	N/A	N/A	variable (0.03102 at 43.9°C)	20.824	1,250
Concrete	N/A	N/A	N/A	1.442	2,248.67	880
No. 15 Felt	N/A	N/A	N/A	4.	715	1,500
OSB	N/A	N/A	N/A	0.101	600	1,800
Expanded Polystyrene	N/A	N/A	N/A	variable (0.0395 at 43.9°C)	21.625	1,250
National Research Council 2004 Spruce	N/A	N/A	N/A	0.087	391.1	1,880
Spray Polyurethane				variable (0.039 at 80°C)	30.4	1,470

[10] As far as can be remembered, 6-in. diameter, 115-VAC fans were used for all the center segments and two 4 in. fans were used in each of the corner segments (Figure 3). A variac was used to regulate the speed of all the induction fans simultaneously, and a setting of 70% of full flow was assumed. Based on these recollections and assumptions and the performance of current fans with these specifications, the estimated total flow rate was about 1,882 cfm.

The insulation thermal conductivities were temperature dependent (a single value is tabulated for reference) as shown in Eq. 1, 2, and 3 for XPS, expanded polystyrene, and closed-cell spray polyurethane foam, respectively.

$$\begin{aligned}&\text{if } T \leq 269.25, k = 0.02567\\&\text{if } T > 269.25 \text{ and } T < 316.45, k = -0.01085 + 0.0001569T + 0.776 \times 10^{-7}T^2\\&\text{if } T \geq 316.45, k = 0.03102\end{aligned} \quad (1)$$

$$\begin{aligned}&\text{if } T \leq 269.25, k = 0.03136\\&\text{if } T > 269.25 \text{ and } T < 316.45, k = -0.01207 + 0.0001518T + 0.353 \times 10^{-7}T^2\\&\text{if } T \geq 316.45, k = 0.0395\ (2)\end{aligned}$$

$$\begin{aligned}&\text{if } T \leq 253.15, k = 0.019\\&\text{if } T > 253.15 \text{ and } T < 353.15, k = 0.019 + 0.0002(T - 253.15)\\&\text{if } T \geq 353.15, k = 0.039\ (3)\end{aligned}$$

where:

$T =$ temperature (K)

$k =$ thermal conductivity (W/m.K)

The soil saturation ratios were calculated from the average measured field moisture content values in test pits that were excavated before module construction commenced. These data are reported in Table 4. The data were digitized from a graph that is the only remaining record (Goldberg et al. 1994), hence the four decimal places. The water table at the FTF was at least 80 ft below grade and is thus not a factor in the calculation of SOG foundation heat transfer (Goldberg and Harmon 2015).

Table 4. Simulation Soil Moisture Conditions

Depth Below Grade (in.)	Soil Saturation Ratio
0.0000	0.7000
15.1531	0.9781
24.1071	0.6930
36.0459	0.1792
47.9847	0.1199
59.9235	0.1401
72.0918	0.2598
84.0306	0.1299
90.000	0.1299

The slab was divided into three heat transfer segments in conformity with the methodology used previously (Goldberg and Steigauff 2013) as shown in Figure 8.

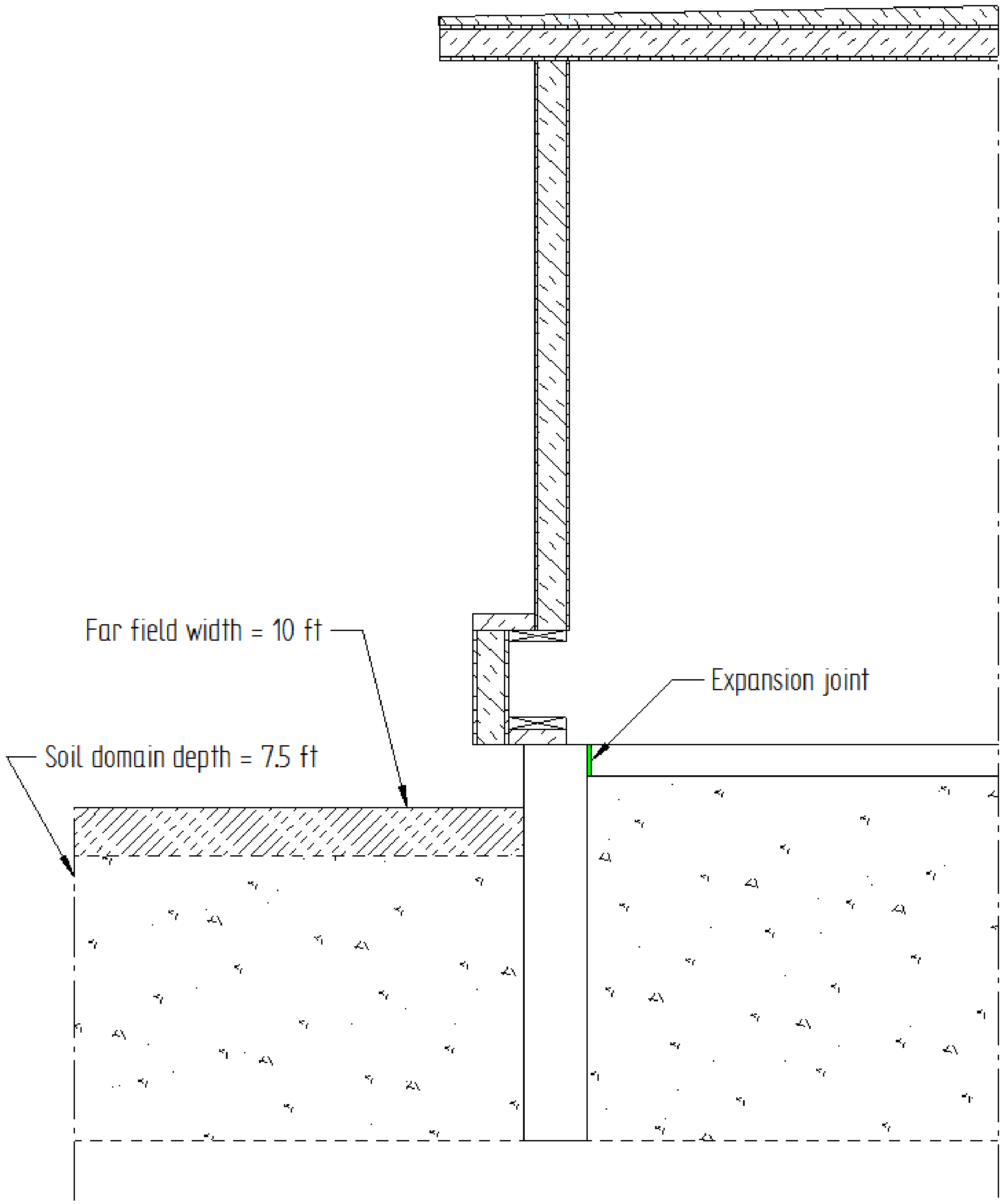

Figure 6. Simulation model of reference module

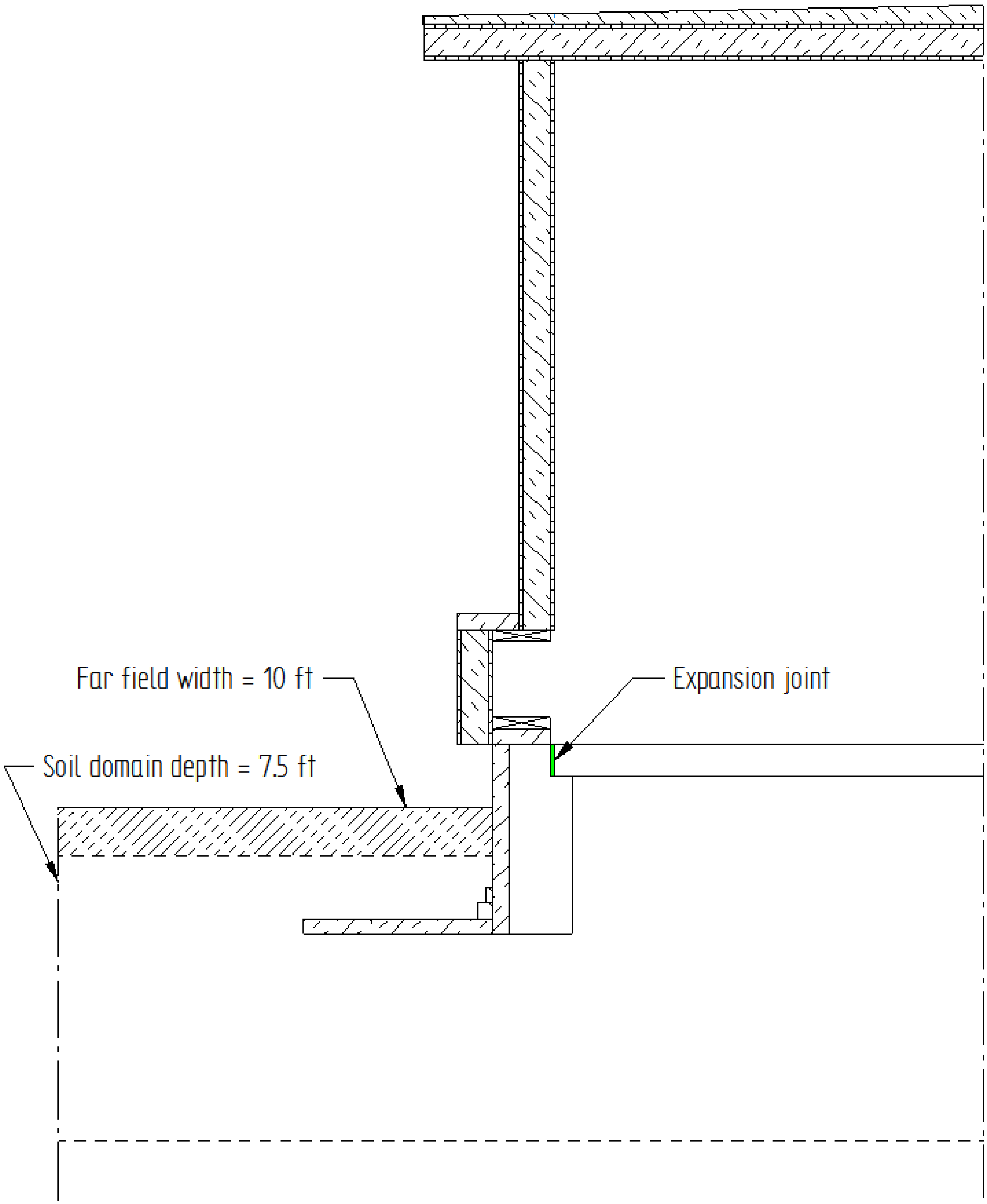

Figure 7. Simulation model of test module

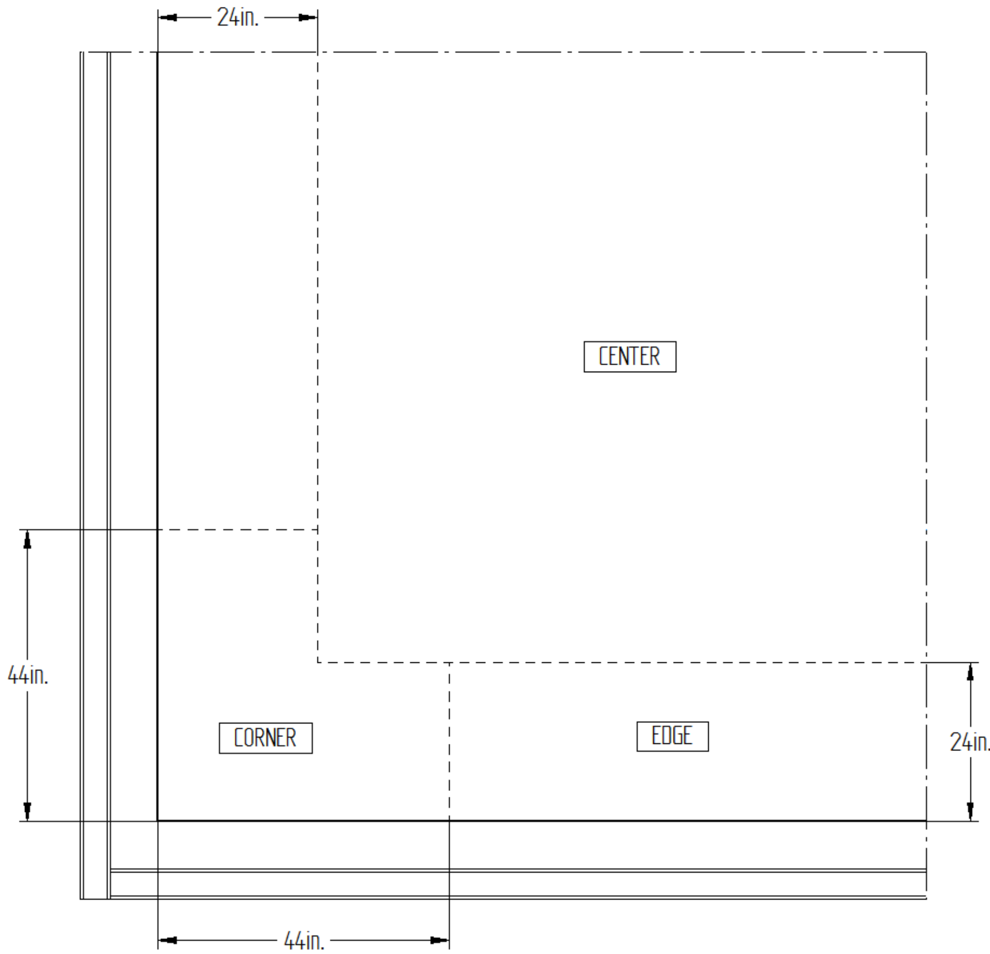

Figure 8. Slab heat transfer sections (one quadrant shown)

The soil domain width was set at 10 ft, which is far larger than the 3.5 ft necessary to capture the heat transport adjacent to the stem wall. The domain depth was made equal to the depth of the test pits at 7.5 ft. Table 5 provides the mesh statistics for the reference and test modules that are based on a tradeoff between spatial resolution and computation period.[11]

Table 5. BUFETS Simulation Domain Mesh Statistics

Module	X-Direction (width) Maximum Control Volumes	Y-Direction (breadth) Maximum Control Volumes	Z-Direction (height) Maximum Control Volumes	Total No. of Active Control Volumes
Reference	37	37	40	34,572
Test	45	45	43	55,844

[11] The computation period increases with mesh density and the chosen mesh size yielded a 48-h run time per simulation case, which was the longest permissible in the project schedule that still permitted adequate spatial resolution.

The larger number of active control volumes for the test module was required to capture the details of the insulation system including the gap protection insulation blocks between the vertical and wing insulation (Figure 7). A standard EnergyPlus weather file based on Typical Meteorological Year 3 data for the Minneapolis-St. Paul Airport weather station was used for the ambient conditions;[12] this weather file does not include any snow depth data (recorded as 0).[13] The simulation commenced on July 1, because only the measured heating season data were included in the comparison. This approach also accelerated the convergence to an annual cyclic steady state. The simulation was initialized by using the EnergyPlus initialization weather record and initial slab surface temperatures to drive the ground and slab temperature field to a steady-state condition. Thereafter the simulation was run for 2 calendar years and the simulation results were reported for the second year. One simulation was run for a third year; the difference between the second and third year slab heat flows on a monthly basis was negligible. The expedited initialization procedure allowed an annual cyclic pseudo steady-state to be reached very rapidly.

Table 6 and Table 7 provide the pseudo steady-state[14] simulation results that correspond to the 1992–1993 experimental data. The durations of the test periods in Table 1 are rounded to the nearest 15 minutes in Table 6, because the BEB simulation time step was 15 minutes.

Table 6. SOG Module Simulation Data

Test Heating Season	Duration	Reference Module (uninsulated)		Test Module (insulated)	
		Site Energy Consumption (kWh)	Slab Heat Flow (kWh)	Site Energy Consumption (kWh)	Slab Heat Flow (kWh)
1992–1993	11/24/1992-16h00 to 4/30/1993-8h45	3,019.85	1,449.12	2,787.98	1,209.75

Table 7. Normalized SOG Module Simulation Data

Test Heating Season	Site Energy Consumption Ratio (γ) (Test/Reference)	Slab Heat Flow Ratio (σ) (Test/Reference)	Reference Module Slab Energy Fraction (β_R) (Slab/Site)	Test Module Slab Energy Fraction (β_T) (Slab/Site)
1992–1993	0.923	0.835	0.480	0.434

Comparing Table 1 and Table 6 shows that the simulation climate was considerably milder than the 1992–1993 experimental climate. (The simulated site energy consumption was lower in both test modules.) A comparison of the ratios in Table 2 and Table 7 reveals that, in the experiment,

[12] The measured ambient data were lost as noted previously.
[13] This does not affect the test/reference model inherent normalization as discussed after Table 1..
[14] Year over year total site energy consumption differs by less than 10%.

the slab accounted for 18% and 11.8% of the whole module energy consumption in the reference and test modules, respectively; in the simulation, the corresponding values were 48% and 43.4%. Hence, either the above-grade simulated structure was considerably more energy efficient than that in the experiment or, more likely, the experimental slab heat flow measurement apparatus had a greater impact on isolating the slab from the room than anticipated, despite the high airflow rate.

Comparing the experimental and simulation γ ratios (site energy comparison) shows a discrepancy of 0.06 or an error of 7% based on the average experimental ratio of 0.863. The simulation is therefore conservative relative to the experiment as it underestimates the energy savings afforded by the stem wall insulation in the test module. Table 8 provides further investigation of the source of the error and shows evaluations of subperiods of the experiment duration.

Table 8. Subperiod Values of Site Energy Ratio

Subperiod	Experimental Site Energy Consumption Ratio (γ) (Test/Reference)	Simulation Site Energy Consumption Ratio (γ) (Test/Reference)	Error (%)
12/17 to 4/4	0.857	0.915	6.8
1/4 to 3/18	0.853	0.908	6.4
1/19 to 3/3	0.852	0.893	4.8
1/19 to 4/4	0.860	0.926	7.7
12/17 to 3/3	0.851	0.893	4.9

Table 9 shows that as April and most of March are removed from the calculation, the error decreases to less than 5%. This implies that the simulation may be overestimating the heat loss through the slab in the test module as spring approaches. With reference to Figure 5, this is most likely a result of the radial slab cavity air temperature gradient in the experiment being different from that in the simulation. In the experiment, the temperature decreases from the perimeter to the center of the slab. In the simulation, the air temperature is uniform across the slab at the mean zone temperature. Thus, the heat loss in the experiment would be less than that in the simulation over the center of the slab in particular, hence the overestimate of the test module heat loss in the center of the slab in the simulation. This can be further examined by comparing the experimental heating season simulated slab heat flows in each of the three slab sections (Figure 8) separately as shown in Table 9.

Table 9. Simulated Slab Quadrant Heat Flow (12/1 to 4/30)

Slab Section	Simulation Reference Module (kWh)	Simulation Test Module (kWh)	Simulated Slab Heat Flow Ratio (σ) (Test/Reference)
Center	68.25	135.87	1.99
Edge	179.87	100.71	0.54
Corner	101.21	57.13	0.56
Quadrant	349.43	293.71	0.84

From Table 2, the experimental value of σ for the entire slab is 0.57, which is close to the values in Table 9 for the corner and edge. It is quite striking that in the simulation of the test module, the center slab heat flow is higher than the edge and corner heat flows; in the reference module simulation, it is lower than the perimeter flows. In other words, the perimeter insulation in the test module is mainly effective at the corners and the edges; the heat loss from the center zone is actually directed away from the deep ground toward the edges, because this offers a lower resistance heat flow path to a thermal sink (a direct consequence of Bejan's Constructal Law, for example, see Bejan and Lorente 2004). This does not occur in the reference module where evidently the lowest heat flow path resistance for heat loss from the slab center is mainly to the deep ground, hence the lower heat flow in the center of the reference module. The heat flow regimes are quite different in frost footing and shallow SOG foundations (discussed further in Section 4).

In the experiment, the incoming air is chilled as it flows over the perimeter zones; thus, the air temperature above the center of the slab is lower and results in a lower center slab heat transfer. This effect likely is substantial in the experimental reference module in comparison with the simulation in which the slab center air temperature is independent of the perimeter insulation and remains constant. This effect can reasonably account for at least part of the 7% underestimate of the site energy savings by the simulation that overestimated the heat loss in the center of the reference module slab.

The major difference in the center slab heat flow likely results in the full slab simulated σ of 0.84 being so much larger than the experimentally measured value of 0.57. Given the differences in slab boundary conditions, the simulation slab heat flows cannot be compared directly against those measured. However, by taking into account the differences between the simulation and experimental values of β_T and β_R, an indirect comparison is possible via the following manipulation.

Given the hypothesis that the site energy consumption ratio γ is constant, then:

$$\frac{E_{M,T,EXP}}{E_{M,R,EXP}} = \frac{E_{M,T,SIM}}{E_{M,R,SIM}} \quad (4)$$

where:

E_M = metered energy
T = test
R = reference
EXP = experimental
SIM = simulation

Noting that:

$$E = \frac{Q_S}{\beta} \quad (5)$$

where:

Q_S = slab heat flow
β = slab energy fraction

Substituting (2) into (1), substituting $\sigma = Q_{S,T}/Q_{S,R}$ and rearranging yields:

$$\frac{\sigma_{EXP}}{\sigma_{SIM}} / \frac{\beta_{R,SIM}}{\beta_{T,SIM}} \frac{\beta_{T,EXP}}{\beta_{R,EXP}} = 1 \qquad (6)$$

Substituting the values from Table 2 and Table 7 yields a ratio for Eq. (6) of 0.938 or an error of 6.2% that is similar to that for the comparison of γ (7%).

Finally, Table 10 shows the impact of different infiltration rates (with all other simulation parameters remaining the same) for the test and reference modules.

Table 10. Effect of Different Test Module Simulation Rates

Case	Reference Module ELA (cm^2)	Test Module ELA (cm^2)	Simulation Site Energy Consumption Ratio (γ) (Test/Reference)	Simulation/ Experiment γ Error (%)
1	14.85	3	0.896	3.8
2	3	14.85	0.953	10.4

Including the uncertainty introduced by a substantial difference in infiltration rates between the test and reference modules bounds the simulation error to 7% –3.2%/+3.4%.

The results of the comparison exercise can be interpreted in two possible ways:

1. The simulation and experimental site energy data are in error by 7% –3.2%/+3.4%. The simulation underestimates the site energy savings provided by vertical and wing stem wall insulation by 3.3% to 9% in absolute terms.
2. The simulation yields site energy savings comparable with those measured. The difference between the simulated and experimental site energy savings may be accounted for by:
    A. The different air temperature profiles above the slab in the experiment and in the simulation
    B. Possibly different infiltration rates in the experimental test and reference modules.

These results point to the need for repeating the experiment with a different approach to measuring the slab heat transfer that more closely replicates the mostly convective heat transfer that occurs in real-world buildings. The results show that the BEB simulation/experiment comparison yields a maximum error of 10.4% distributed over errors in both EnergyPlus and BUFETS-B as well as uncertainty in the experimental infiltration rates. However, there is no reason to suppose that using the simulation to assess the relative performance of different SOG insulation strategies across differing climates yields a 10.4% error, because the same absolute error would apply to all cases. This error also may imply an underestimate of the site energy savings and thus an overestimate of the payback period, but likewise, these estimation errors would apply to all cases. In keeping with this philosophy that was used in the previous major study of SOG foundation insulation energy performance (Labs et al. 1988), the SOG insulation performance assessment reported in the following sections was undertaken.

4 Insulation Optimization

4.1 Development of the Optimization Module

Following the test plan, the experimental reference module with a conventional footing was adapted to yield a building that is useful for conducting the foundation insulation optimization process in a zone 6 climate (Minneapolis, Minnesota). The key requirement in the adaptation was to maximize the slab heat flow/site energy ratio (β). This allowed changes in the stem wall insulation system to maximize the resultant site energy consumption changes. Thus the signal-to-noise ratio[15] of the insulation changes was maximized. The other consideration was to make the optimization module more like an actual residential building. The development of the optimization module is discussed with reference to the simulation results compiled in Table 11. The optimization module (Figure 9) was derived from the reference module (Figure 6) by making the following changes:

- Adding a standard exterior wooden door
- Removing the guard cavity at the base of the walls
- Increasing the ELA to represent an infiltration level of typical of new construction in 2000.

Table 11. Optimization Module Development

Module	ELA (cm^2)	Annual Slab Center Heat Flow (kWh)	Slab Energy Fraction (β) (Slab/ Site)	Slab Heat Flow Ratio (σ) (Insulated/ Base)	Site Energy Consumption Ratio (γ) (Insulated/ Base)
Experimental Reference Module	3	281.217	0.480	N/A	N/A
Experimental Test Module	3	558.960	0.434	0.835	0.923
Optimization Module (No Windows)	36.8	402.520	0.511	N/A	N/A
Optimization Module (No Windows) +2012 IECC SOG Insulation	36.8	278.424	0.322	0.474	0.753
Optimization Module + 4 Windows	36.8	417.068	0.527	N/A	N/A
Optimization Module + 4 Windows +2012 IECC SOG Insulation	36.8	280.309	0.336	0.462	0.724

The balance of the reference module was unchanged; that is, the structure (2 × 4 SIPs) and size were the same as those used in the experiment (see Figure 2).

[15] A measure of the signal strength relative to the signal noise.

From Table 11 these changes increased β from 0.480 for the reference module to 0.511 for the optimization module; that is, more than half the enclosure energy load was attributable to slab heat flow. Adding 2012 IECC required stem wall insulation (R-10 from the top of the stem wall to the top of the footing) to the optimization module yielded a site energy consumption ratio (γ) of 0.753 (site energy savings of 24.7%) compared with the 7.7% realized for the simulated experimental test module (with a shallow FPSF). The increase in energy savings provides the required higher signal-to-noise ratio necessary for insulation optimization purposes. The reason for the significantly higher savings for the insulated optimization module compared with the experimental test module may be inferred by examining the slab center heat flow data for the experimental and optimization modules. In the case of the experimental modules, adding shallow stem wall and wing insulation to the experimental test module increased the slab center heat flow by a factor of 1.99. However, in the case of the optimization module with no windows, adding 2012 IECC-required insulation to the frost footing stem wall decreased the slab center heat flow by a factor of 0.69. The difference resulted from the difference in slab surface heat transfer mechanisms discussed in Section 3. For both module types, the corner and edge heat flows decreased on average by 0.56 for the experimental test module and by 0.42 for the insulated base optimization module. Hence the slab heat transfer regime for a SOG FPSF is very different from that of a conventional frost footing SOG foundation owing to the effect described by the Constructal Law (discussed in Section 3). This difference magnifies the impact of stem wall insulation with a frost footing, because it does not yield the increase in slab center heat flow that occurs with a FPSF.

The final modification was to add solar gain to the slab of the optimization module by adding four standard[16] "Tilt-Wash" windows (each 56.875 in. tall by 25.625 in. wide) to the south wall. This addition allowed the optimization module to more closely resemble an actual SOG home and increased β to 0.527 for the uninsulated case. Adding 2012 IECC-required stem wall insulation further decreased γ to 0.724 for a site energy savings of 27.6% that was deemed sensitive enough for SOG insulation optimization purposes. The resulting optimization module is shown in Figure 9. The optimization module with four windows and no slab insulation was used as the uninsulated reference for all the SOG foundation insulation strategies tested.

[16] Andersen Windows Inc. model no. TW2042.

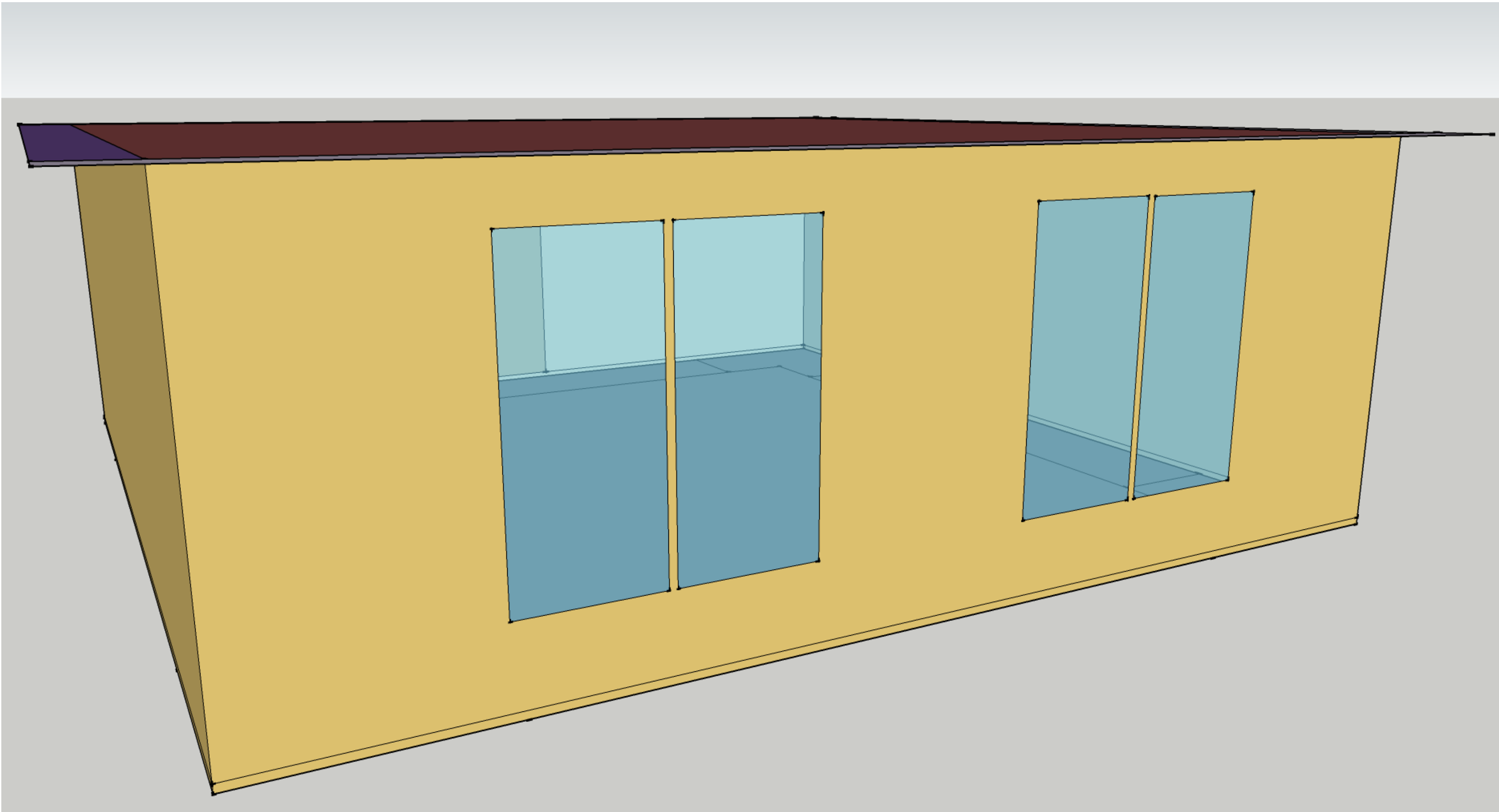

Figure 9. Optimization module

4.2 Insulation Strategies Evaluated

On the basis of the test plan, ten insulation strategies were developed and tested against an uninsulated base case to compare their thermal effectiveness.[17] These strategies are shown in Figure 10. Options a through i use hydro-vacuum excavation in an application that was developed by Northern*STAR* (Schirber et al. 2014) to form a trench just wide enough to allow installation of insulation materials. Options a and b employ sheets of XPS foam placed against the wall as the insulating layer. Option b corresponds to the 2012 IECC requirement for SOG foundations in zone 6. Options c through i use a layer of 1- or 2-in. XPS as an insulating form for poured polyurethane (PPU), which is placed behind the foam against the wall. This method is likely to result in a more consistent thermal control layer, because it has no seams. XPS is less expensive than PPU, so this method is expected to be more cost-effective than simply filling the entire trench with PPU.

Options e through g are schemes that take advantage of the fact that the hydro-vacuum process can cut relatively precise angles in the soil. These use a tapered trench. The advantage of tapered insulation is that the thermal effectiveness of the installed insulation increases with decreasing depth below grade. That is, the thermal effectiveness of the insulation system as a whole increases if the insulation thickness decreases with depth below grade.

[17] Thermal effectiveness is defined as the ratio: one-dimensional heat flux/three-dimensional heat flux for the same thermal resistance.

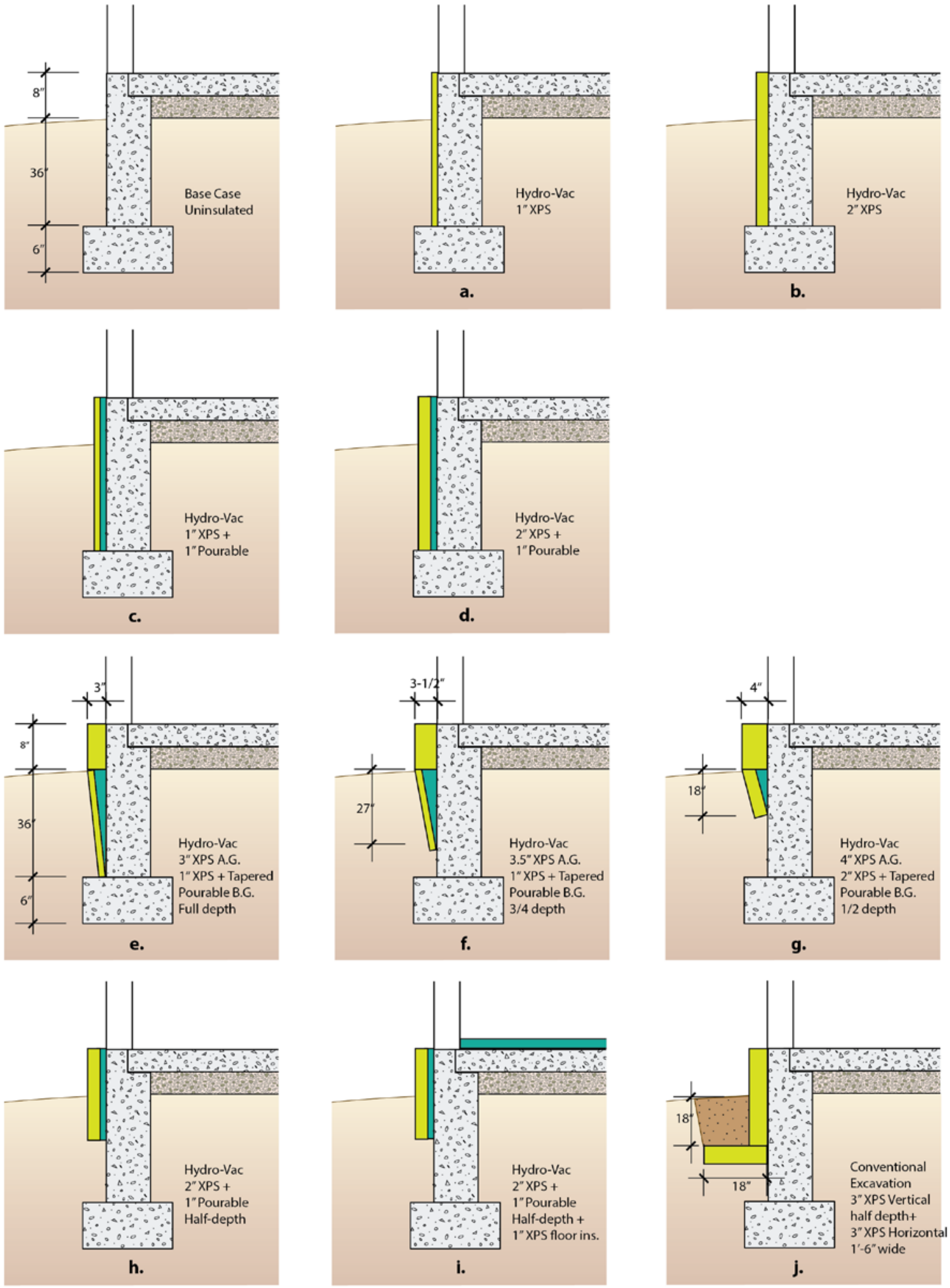

Figure 10. Foundation insulation upgrade designs

After excavation, 1- or 2-in. XPS is placed against the sloping trench wall, and PPU is placed in the tapered gap between the XPS and the stem wall. XPS is fixed to the above-grade part of the wall as a second operation. The variables explored in these options are depth and above-grade insulation thickness; as depth decreases, thickness increases. Options h and i are variations on option d but are installed to half the depth of the stem wall. Option i includes 1 in. of XPS applied to the entire floor on the interior of the house. Option j shows a conventional FPSF insulation upgrade.

4.3 Simulated Energy Performance of the Insulation Strategies

The BEB simulation methodology described above was used to simulate the energy savings of the ten insulation upgrade options. Minneapolis Typical Meteorological Year climate data were used for the analysis. Given the heating-dominated climate at that location, the analysis period was limited to the heating season because, in a zone 6 climate, SOG perimeter insulation decreases site energy consumption during the heating season only. During the cooling season, this insulation increases the site energy consumption (see Table 36 for a single-family dwelling example). Figure 11 summarizes the whole-building site energy savings results. (Appendix A gives the detailed simulation results.)

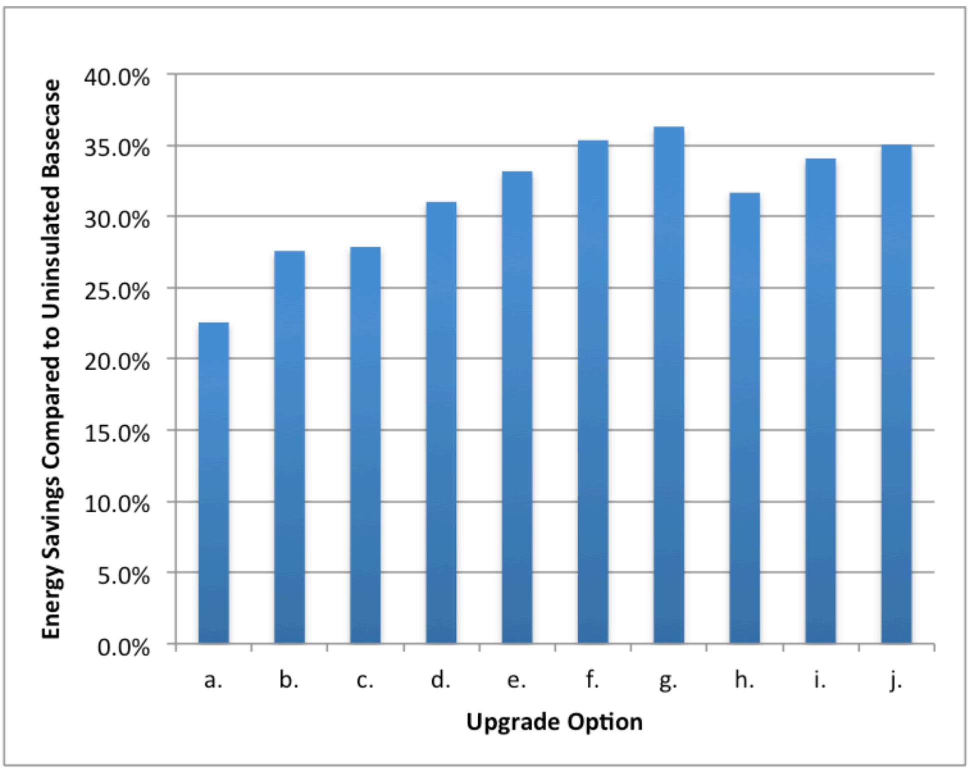

Figure 11. Foundation insulation upgrade design modeled site energy savings

The incremental R-value in options a through d produce incremental energy savings, as expected. Options e, f, and g show increasing energy savings with the use of tapered insulation. These savings are a function of increasing the insulation thickness near the top of the wall, where temperatures are coldest during the heating season. Option g has the best energy savings of any configuration modeled. Option i shows energy savings between options e and f (but less than g);

however, the continuous interior floor insulation will make this approach unfeasible in an occupied home. Option j nearly matches f for thermal performance, but its horizontal "wing" insulation means a disruptive (and costly) trench must be dug.

4.4 Cost-Effectiveness of the Insulation Strategies

Cost models were developed to assess the cost-effectiveness of each strategy. Combined labor and material costs developed by Schirber et al. (2014) were used for hydro-vacuum excavation and PPU foam installation. Both of these costs are strongly related to material volume. The cost of XPS was obtained from a local contractor supply house, and a 10% markup was applied to the wholesale cost. Miscellaneous labor was generally charged at three times the material cost; however, labor costs are similar for similar operations. For instance, labor costs are the same to install 1-in. XPS as to install 2-in. XPS. The costs exclude the above-grade flashing and trim (Table 12).

Table 12. Insulation Upgrade System Costs per Linear Foot

Module	Excavation	XPS	PPU Foam	Labor	Floor Foam (option i only, 5 ft^2 per linear foot)	Total Cost per Linear Foot
a.	$4.83	$2.27	$0.00	$6.81	$0.00	$13.91
b.	$7.21	$3.92	$0.00	$6.81	$0.00	$17.94
c.	$7.21	$2.27	$5.51	$6.81	$0.00	$21.80
d.	$9.66	$4.33	$5.51	$6.81	$0.00	$26.31
e.	$4.83	$2.93	$4.50	$9.09	$0.00	$21.35
f.	$3.62	$2.79	$4.21	$8.37	$0.00	$18.99
g.	$3.22	$2.48	$3.37	$7.44	$0.00	$16.51
h.	$4.83	$2.56	$3.26	$4.03	$0.00	$14.68
i.	$9.66	$4.33	$5.51	$6.81	$12.40	$38.71
j.	$38.76	$7.00	$0.00	$14.76	$0.00	$60.52

4.5 Selection of the Optimized Insulation Strategy

This study required the selection of one strategy to apply to two prototype buildings in four climates on the assumption that the optimized strategy selected for the heating season in zone 6 is applicable to zones 4, 5, and 7 as well. Although the assumption is reasonable for zone 7, and likely satisfactory for zone 5, it may not be true or cost-effective for zone 4. Thus, as discussed in Section 5.3, a different strategy was used in zone 4 because a tapered insulation trench with a very shallow frost footing depth is impractical. A further constraint was imposed by the test plan because of the amount of time to run a BEB simulation for any particular case (generally 48–96 hours). This allowed for only one simulation per building type in each climate, so individual foundation insulation optimizations in each climate were not possible. The authors acknowledge that this methodology may not have identified the theoretically optimum solution in climate zones other than the one used (zone 6A).

To identify the most cost-effective solution, installation costs were compared to annual energy savings, in megawatt-hours (MWh). Table 13 shows the summary, including the total site energy savings. Option g shows the highest energy savings, along with the lowest cost per MWh saved. In addition, overall cost is the third-lowest among the options considered. Option h is also a strong contender. Its first cost is significantly less than g, and cost per MWh saved is nearly identical to g. Absolute site energy savings are smaller, however; the results for h land in the middle of the pack. Because of its lowest cost per unit energy saved, and its highest total energy saved, option g was chosen for simulation in the prototype buildings in four climates.

Table 13. Insulation Upgrade Systems Cost-Effectiveness

Configuration	Total Cost per Linear Foot	MWh Savings	Cost per MWh Saved
a.	$13.91	0.89	$15.60
b.	$17.94	1.09	$16.46
c.	$21.80	1.10	$19.79
d.	$26.31	1.23	$21.46
e.	$21.35	1.31	$16.29
f.	$18.99	1.40	$13.59
g.	$16.51	1.43	$11.51
h.	$14.68	1.25	$11.73
i.	$38.71	1.35	$28.74
j.	$60.52	1.39	$43.69

The slab heat flow data were calculated separately for the corners and the perimeter between the corners. For example, from Table 35 for a single-family dwelling in zone 7, the slab heat flow energy savings at the corners and center edges were 43.5% and 46.5%, respectively. Because the center edge savings are 3% greater than the corner savings, changing the slab width/length ratio in a way that increases the center/corner perimeter length ratio increases the slab heat flow savings and vice versa.

5 Optimized Insulation Configuration Performance for Four Climates

5.1 Climate Selection

Climate zones from mixed-humid (M-H) to very cold/cold (VC/C) were chosen because of the increased likelihood of cost-effectiveness compared to warmer climates. This likelihood is driven by a pronounced heating season during which the temperature difference between inside and outside is greater than in cooling-dominated climates. Therefore, more thermal energy moves through enclosure components than in milder climates. The area of interest coincides with IECC climate zones 4–7.

The Northern*STAR* team consulted the 2009 Residential Energy Consumption Survey, published by the U.S. Energy Information Administration (EIA 2009a). This survey shows the following:

- States within climate zones 4–7 were chosen because they contained large numbers of houses built on SOG foundations, and because they were isolated in the EIA data.
- These data often combine multiple states into one statistical category, which often includes more than one climate zone. For these reasons, Virginia (zone 4), Ohio (zone 5), and Wisconsin (zone 6) were chosen.
- Ohio is combined with Indiana in the data; however, all the major population centers are in zone 5.
- Duluth, Minnesota, was chosen as the largest population center in zone 7, even though Minnesota is combined with Iowa, North Dakota, and South Dakota in the EIA data (zones 5, 6, and 7).
- Cities in Virginia, Ohio, and Wisconsin were chosen that were significant population centers and therefore likely to have a large population of houses built on SOG foundations.

Reports within the EIA survey (EIA 2009b) describe the number of housing units with a particular foundation type, delineated by Building America climate zone designations.

- Overall, the VC/C climate zones have 38.8 million housing units; the M/H climate zones have 35.4 million.
- Of these, 9 million in VC/C and 11.3 million in M/H report "concrete slabs" as the primary foundation type. This represents 23.2% in VC/C, and 31.9% in M-H, or 27.4% overall.

These data can be correlated with other survey reports (EIA 2009c) that break up the housing numbers by year of construction, again by Building America climate zones.

- The survey reports 113.7 million housing units in the VC/C and M-H climate zones.
- Of these, 33.5 million, or 29%, were built before 1970.

- Assuming the proportion of slab foundations to all houses is consistent with time, these climate zones have 9.2 million housing units on slab foundations that were built before 1970.

This is meaningful because houses built before 1970 on concrete slab foundations were unlikely to include significant slab insulation, which makes them candidates for insulation upgrades. Even in Minnesota, a state-level code that addresses energy efficiency was not adopted until 1976 (MN DLI 2012). In addition, materials that are suitable for use as below-grade insulation were generally unavailable until about the same time (Dow 2014). Also, slab foundations probably continued to be uninsulated after 1970, especially in warmer climates, so this estimate can be considered conservative.

5.2 Simulation Parameters

In recent research, the predictions of the BUFETS simulation code were compared against detailed transient experimental data for full basement walls with different soil and moisture conditions in a zone 7 climate (Goldberg and Harmon 2015; Harmon 2014). In accordance with the results of this research, the following location-specific geometrical parameters and boundary conditions are crucial for achieving an accurate simulation:

- Depth of the frost footing
- Depth of the water table beneath the footing
- Depth of the soil domain beneath the footing
- Steady-state soil temperature at the base of the soil domain.

The frost footing depths are listed in Table 14 and were determined either from the relevant state statutes (if available) or from local city or county building codes.

Table 14. Frost Footing Depths

Location	Zone	Footing Depth (in.)	Reference
Duluth, MN	7	60	MN Statutes, 1303.1600.1
Madison, WI	6	48	WI Statutes, SPS 321.16
Cleveland, OH	5	42	City of Cleveland, Climatic and Geographic Design Criteria[18]
Richmond, VA	4	18	Building Codes for Richmond, VA[19]

The groundwater height (or water table height) was determined from the Active Groundwater Level Network maintained by the U.S. Geological Survey (USGS)[20] for zones 4–6 (shown in Table 16, Table 17, and Table 18, respectively). However the USGS has no observation wells in Duluth, Minnesota (zone 7). In this case, the groundwater height was determined from the Minnesota County Well Index maintained by the Minnesota Department of Health[21] (Table 15). In all cases, the results from five observation wells were tabulated, and the average of the three shallowest wells was used to represent the water table height in each zone.

[18] http://portal.cleveland-oh.gov/clnd_images/Buildinghousing/ClimacticGeograDesign.pdf
[19] http://www.richmondgov.com/planninganddevelopmentreview/PermitsInspectionsBureau.aspx
[20] http://groundwaterwatch.usgs.gov/default.asp
[21] http://mdh-agua.health.state.mn.us/cwi/cwiViewer.htm

Table 15. Groundwater Depths for Duluth, Minnesota (Zone 7)

Well No.	Depth (ft)	Observation Period
739041	10	10/10/2007
703163	10	5/4/2007
559186	7	9/28/2004
483739	5	20/5/1992
704829	4	8/28/2009
Average of 3 Lowest	5.33	

Table 16. Groundwater Depths for Madison, Wisconsin (Zone 6)

USGS Site No.	Minimum Depth (ft)	Maximum Depth (ft)	Average Depth (ft)	Observation Period
430429089230301	79.1	130.7	104.9	7/21/1946–6/2/2014
430456089190603	41.6	65.37	53.49	5/8/2008–8/26/2014
430427089284901	44.94	58.82	51.88	1/1/1938–8/26/2014
430406089232901	13.05	23.05	18.05	11/10/1978–8/26/2014
430718089291501	15.33	19.81	17.57	2/8/2010–9/10/2014
Average of 3 Lowest			29.17	

Table 17. Groundwater Depths for Cleveland, Ohio (Zone 5)

USGS Site No.	Minimum Depth (ft)	Maximum Depth (ft)	Average Depth (ft)	Observation Period
412748081172000	87.89	92.36	90.13	2/29/1996–8/6/2014
412541081194500	56.73	62.22	59.48	1/5/2001–8/6/2014
413247081103300	24.13	27.18	25.66	2/27/1996–8/7/2014
413138081152000	21.17	25.29	23.23	6/15/1978–8/6/2014
412331081123000	11.34	14.34	12.84	6/8/1978–8/6/2014
Average of 3 Lowest			20.58	

Table 18. Groundwater Depths for Richmond, Virginia (Zone 4)

USGS Site No.	Minimum Depth (ft)	Maximum Depth (ft)	Average Depth (ft)	Observation Period
373428077233001	186.13	197.63	191.88	1/7/1988–7/23/2014
372936077211101	60	147.53	103.77	1/23/1972–6/2/2014
373817077282501	3.37	18	10.69	7/15/1977–7/21/2014
363607077331401	1.48	10.45	5.97	5/20/1969–7/21/2014
372519077264605	-1.64	9.12	3.74	5/22/1985–7/21/2014
Average of 3 Lowest			6.8	

Following Harmon (2014), a physically appropriate minimum water table height above the base of the soil domain is 8 ft if the water table is 4 ft or less below the footing.[22] In general,

[22] This arises because a water table close to the footings creates a very high-capacity thermal source/sink that significantly changes the heat flow around insulated foundation walls.

simulation accuracy with respect to matching the measured and simulated soil temperatures adjacent to an insulated basement foundation wall increases with the depth of the soil domain beneath the footing. With reference to Table 15 through Table 18, the water table depths range from a minimum of 5.33 ft for Duluth, Minnesota, to a maximum of 29.17 ft for Madison, Wisconsin. Therefore, to keep the soil domain height constant for all climates and maintain the top of the water table above the base of the soil domain, the domain depth was set at 30 ft below grade. With this grade depth, the water table height criterion is met for all climates (Table 19).

Table 19. Water Table Geometry

Location	Zone	Depth of Water Table beneath Footing (ft)	Height of Water Table above Base of Soil Domain (ft)
Duluth, MN	7	0.33	24.67
Madison, WI	6	25.17	0.83
Cleveland, OH	5	17.08	9.42
Richmond, VA	4	5.33	23.17

The Dirichlet temperature boundary condition at the base of the soil domain was taken to be the deep well water temperature (Table 20).[23] These temperatures are given by Labs et al. (1988), who in turn sourced the data from a contour map published by the National Well Water Association (which appears to be extinct). More recent data for well water temperatures could not be found in the literature.

Table 20. Well Water Temperatures

Location	Zone	Temperature (°F)
Duluth, MN	7	48
Madison, WI	6	51
Cleveland, OH	5	53
Richmond, VA	4	60

For consistency with the validation and optimization simulation sets, the soil and foundation material properties were the same as those used in Section 3 and Section 4 (Table 3). However, the soil saturation ratio profiles shown in Table 4 were modified to account for the height of the water table (Table 21). The saturation ratio was set to unity at the surface of the water table and the values from that surface upward were taken from Table 4.

[23] Average groundwater temperature data are not appropriate because they are measured too close to the surface.

Table 21. Far Field Soil Saturation Ratio Profiles

Zone 4		Zone 5		Zone 6		Zone 7	
Depth Below Grade (in.)	Soil Saturation Ratio	Depth Below Grade (in.)	Soil Saturation Ratio	Depth Below Grade (in.)	Soil Saturation Ratio	Depth Below Grade (in.)	Soil Saturation Ratio
0	0.7000	0	0.7000	0	0.7000	0	0.7000
15.1531	0.9781	15.1531	0.9781	15.1531	0.9781	15.1531	0.9781
24.1071	0.6930	24.1071	0.6930	24.1071	0.6930	24.1071	0.6930
36.0459	0.1792	36.0459	0.1792	36.0459	0.1792	36.0459	0.1792
47.9847	0.1199	47.9847	0.1199	47.9847	0.1199	47.9847	0.1199
59.9235	0.1401	59.9235	0.1401	59.9235	0.1401	59.9235	0.1401
72.0918	0.2598	72.0918	0.2598	72.0918	0.2598	64	1
78	0.1299	84.0306	0.1299	84.0306	0.1299	360	1
82	1	90	0.1299	90	0.1299		
360	1	243	0.1299	346	0.1299		
		247	1	350	1		
		360	1	360	1		

5.3 Design of the Single- and Multifamily Test Homes

Three housing unit types were designed as test beds for energy modeling in climate zones 4–7:

- A single-story single-family home
- A two-story multifamily end unit (attached wall on one side)
- A two-story multifamily center unit (attached walls on two sides). The whole multifamily building consisted of a combination of two center and two end units.

The models were developed in BEopt, then exported for detailed foundation heat flow modeling using the BEB protocol.

All designs enclose 1,800 ft^2 of living space. The single-story single-family home has a footprint of 30 ft × 60 ft. The multifamily units are two-story with a footprint of 20 ft × 45 ft. Whole-building analysis for the multifamily unit used two end units and two center units to generate a four-unit building.

The Building America B10 Benchmark default inputs were used with a few exceptions to more accurately reflect the characteristics of existing homes. Table 22 shows the parameters that were adjusted.

Optimized insulation configuration g was used in all cases except Richmond, Virginia. This configuration consists of insulating to 1/2 the below-grade depth of the stem wall. Two-inch XPS is placed against the sloped trench wall, leaving a 2-in. inch space between the XPS and foundation wall at grade. The tapered space between the XPS and foundation wall is filled with PPU foam.

Table 22. Adjustments to B10 Benchmark Inputs

Component Name	B10 Benchmark	Zone 4 and 5 Inputs	Zone 6 and 7 Inputs
Exterior Walls	Uninsulated	R7 fiberglass, grade 1	R7 fiberglass, grade 1
Attic Floor	R11	R19.6 fiberglass	R25 fiberglass
Windows	1 pane clear, metal frame	2 pane clear, nonmetal frame	2 pane clear, nonmetal frame
Air Leakage	15 ACH50	7 ACH 50 (3 ACH 50 for multifamily)	7 ACH 50 (3 ACH 50 for multifamily)
Ducts	20% leakage, R4, in unconditioned attic	Inside conditioned space	Inside conditioned space

In Richmond, the optimized zone 6 SOG insulation strategy was not applied because of the shallowness of the frost footing and no Richmond-specific optimizations were performed. Instead, two insulated cases were modeled, both with 4-in. XPS below-grade insulation: one full-depth (10.75 in. below grade to the top of the footing) and one half-depth (5.375 in. below grade). The shallow foundation depth in Richmond meant that the advantages of the tapered insulation approach seen in deeper applications were minimized; therefore, a less-costly application of vertical XPS with no PPU foam was substituted. The part of the foundation wall that is exposed above grade is covered with 4 in. of XPS in all cases. Table 23 shows the itemized and whole-system costs for the systems modeled.

Table 23. System Cost by Climate

City	Excavation Cost	XPS	PPU Foam	Labor	Total Cost per Linear Foot	Single-Family System Cost (180 linear feet)	Multifamily System Cost (250 linear feet)
Duluth	$3.22	$3.77	$2.20	$7.44	$16.63	$2,993.90	$4,158.20
Madison	$2.44	$3.24	$1.70	$5.75	$13.13	$2,363.00	$3,281.95
Cleveland	$2.10	$2.97	$1.45	$4.90	$11.42	$2,055.65	$2,855.07
Richmond Half Wall	$0.66	$1.90	N/A	$1.51	$4.07	$733.03	$1,018.09
Richmond Full Wall	$1.31	$2.38	N/A	$3.03	$6.72	$1,209.90	$1,680.41

5.4 Single-Family Home Energy Results and Retrofit Cost-Effectiveness

Eighteen model runs were conducted using the BEB simulation protocol. Each run represents a full year of heating and cooling energy use. Nine runs were conducted for the single-family case and 18 for the multifamily case (nine each for the end and center units). A baseline uninsulated case was run for each housing type in each climate, in addition to the optimal insulation case. Figure 12 shows the energy savings for the single-family home relative to the uninsulated case (the detailed simulation results are given in Appendix B). The reduction of energy flow through the foundation is substantial, ranging from 13.8% for half-wall insulation in zone 4 to 31.4% in zone 7; that is, the savings increase markedly as the climate becomes colder. However, the site and source energy savings are modest. This is because a small fraction of the total building thermal load occurs through the foundation in the modeled houses (maximum value of 14.1% for an uninsulated slab in zone 7).

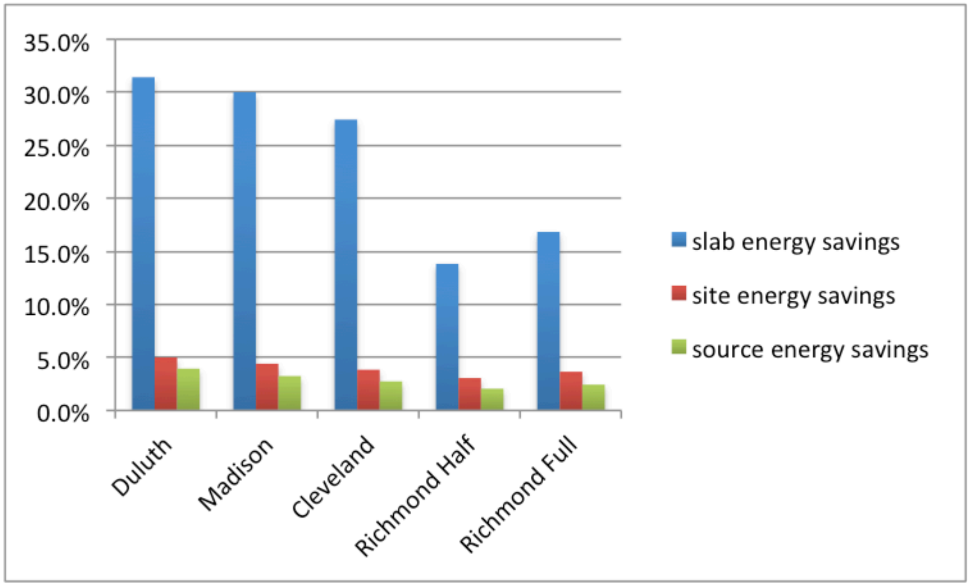

Figure 12. Single-family home energy savings

The effect of the SOG insulation on the contiguous cooling load[24] is shown in Table 24. In Madison and Duluth, the insulation increases the cooling load slightly (3.2% maximum in Duluth). This arises because the SOG insulation decouples the slab from the cool ground yielding a warmer slab surface in the cooling season and thus an increased cooling load. In Richmond and Cleveland, the foundation insulation actually decreases the cooling load by a small amount with a maximum decrease of 1.59% for full wall insulation in Richmond.

Table 24. Effect of Insulation on Single-Family Home Cooling Load

Location/Insulation	Contiguous Cooling Period	Cooling Energy Consumption Change with SOG Insulation (%)
Duluth/Optimized	6/24–9/1	+3.20
Madison/Optimized	6/23–8/1	+0.34
Cleveland/Optimized	6/8–9/5	–.19
Richmond/Half-Wall	6/15–9/10	–1.46
Richmond/Full-Wall	6/15–9/10	–1.59

To assess cost-effectiveness, electricity and gas energy use data were used to determine utility cost data. Regional average costs for electricity and gas service were obtained from the EIA data sets (EIA 2014a, 2014b). Table 25 shows utility rates used to monetize energy savings.

Table 25. Regional Average Gas and Electricity Costs

	Ohio	Wisconsin	Minnesota	Virginia
$/kWh	$0.1225	$0.1462	$0.1277	$0.1208
$/therm	$0.92	$0.84	$0.80	$1.14

[24] This is defined to be the contiguous period during which the cooling plant only operates, the heating plant is dormant.

These monetized energy savings are used to calculate simple payback by dividing the installed cost of the insulation upgrade by the energy savings. Results for the single-family case are shown in Table 26. The annual cost savings are modest, but increase in colder climates. However, due to decreased costs associated with the retrofit in zone 4 (Richmond), payback times are shortest in warmer climates.

Table 26. Energy Cost Savings and Simple Payback—Single-Family Home

	Electricity Savings ($)	Gas Savings ($)	Total Savings ($)	Simple Payback (Years)
Duluth	$6.64	$59.38	$66.01	45.4
Madison	$4.90	$47.15	$52.05	45.4
Cleveland	$3.58	$40.08	$43.66	47.1
Richmond Half Wall	$4.31	$30.14	$34.45	35.1
Richmond Full Wall	$4.95	$36.06	$41.02	17.9

5.5 Multifamily Home Energy Results and Retrofit Cost-Effectiveness

Figure 13 shows energy savings for the whole multifamily building case (the detailed simulation results are shown in Appendix C). The relationship between the slab energy savings and site/source energy savings are similar to the single-family case, though the values are lower. This is because of the increased ratio of occupied space to perimeter foundation length. Because each unit has a lower amount of exposed foundation wall with respect to its occupied area, the energy impact of insulating that foundation wall is decreased.

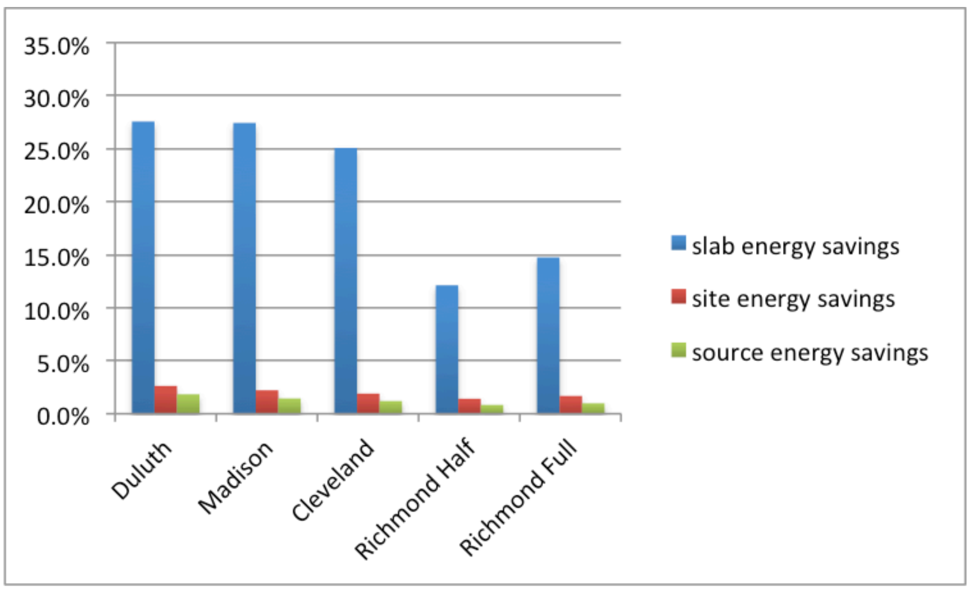

Figure 13. Multifamily home energy savings

The effect of the SOG insulation on the contiguous cooling load for the whole multifamily building case is shown in Table 27. In Madison, Duluth and Cleveland the insulation increases the cooling load a little (3.17% maximum in Duluth). The foundation insulation decreases the cooling load (maximum decrease of 0.23% for half wall insulation) in Richmond alone. The contiguous cooling period is longer for the center units in all cases except Duluth. This arises because the heat loss through the enclosure is reduced significantly by the nominally adiabatic party walls, so that cooling is required earlier in the season.

Table 27. Effect of Insulation on Multifamily Home Cooling Load

Location/Insulation	Center Unit Contiguous Cooling Period	End Unit Contiguous Cooling Period	Cooling Energy Consumption Change with SOG Insulation (%)
Duluth/Optimized	6/23–9/4	6/24–9/2	+3.17
Madison/Optimized	5/26–9/3	6/15–9/9	+0.73
Cleveland/Optimized	5/24–9/28	6/3–9/5	+0.46
Richmond/Half-Wall	5/6–10/2	6/15–9/29	–0.23
Richmond/Full-Wall	5/6–10/2	6/15–9/29	–0.22

Table 28 shows the energy cost savings and simple payback calculations for the multifamily cases. In a pattern that parallels the single-family cases, total energy savings are greatest in cold climates. Because the building has four units, and the perimeter is much longer than in the single-family cases, the absolute dollar savings are greater. However because of the aforementioned increased floor area to perimeter length ratio, payback periods are longer than the single-family cases.

Table 28. Energy Cost Savings and Simple Payback—Multifamily Building

	Electricity Savings ($)	Gas Savings ($)	Total Savings ($)	Simple Payback (Years)
Duluth	$5.55	$85.74	$91.29	45.6
Madison	$2.98	$67.40	$70.38	46.6
Cleveland	$2.66	$57.60	$60.26	47.4
Richmond Half Wall	$3.60	$42.21	$45.81	36.7
Richmond Full Wall	$4.59	$50.41	$55.01	18.5

5.6 Nonenergy Benefits

In addition to energy savings, foundation insulation can confer other benefits. Specifically, insulating the perimeter typically increases slab temperatures in the winter. This increases thermal comfort because of the warming of the slab surface that exchanges radiant heat with the bodies of the occupants. The comfort is assessed in terms of the time that occupants would not be comfortable according to the simple model of ASHRAE Standard 55-2004 as calculated by EnergyPlus (Table 29). The comfort improvement (decrease in discomfort time) as a result of SOG foundation insulation increases from 3.6% in zone 7 to 8.3% in zone 4 with full wall SOG insulation. Thus the comfort improvement increases with the warmth of the climate.

In addition, cold slabs can cause water vapor to condense if their temperature is lower than the dew point of the ambient air. This is exacerbated if carpet is installed on the slab (as was the case on the simulated buildings). Any increase in slab surface temperature will decrease the likelihood of slab surface condensation.

Table 29 EnergyPlus Comfort Performance

Zone: Insulation Configuration	Time Not Comfortable by Simple ASHRAE Standard 55-2004 (Hours)	Comfort Improvement (%)
Zone 7: No SOG Insulation	4,669.00	
Zone 7: with SOG Insulation	4,501.75	3.6
Zone 6: No SOG Insulation	3,979.50	
Zone 6: with SOG Insulation	3,794.25	4.7
Zone 5: No SOG Insulation	3,224.50	
Zone 5: with SOG Insulation	3,046.75	5.5
Zone 4: No SOG Insulation	2,207.25	
Zone 4: with Half Wall SOG Insulation	2,056.25	6.8
Zone 4: with Full Wall SOG Insulation	2,023.50	8.3

Slab surface temperatures were output by the simulations. These are generated for each slab zone (corner, edge, or center) at 15-minute intervals. These data were used to compare slab surface temperatures in the insulated and uninsulated single-family cases in each climate. The northeast corner zone was chosen, as it was found to be the coldest, therefore most problematic, zone in the data. It should be noted that conditions immediately adjacent to the exterior wall may be significantly colder in winter than the data suggest. This is because each data point represents an average of surface temperatures across any particular slab zone. Therefore these results can be considered conservative, with respect to the prediction of conditions that would be conducive to mold growth or moisture accumulation.

Figure 14 through Figure 17 show plots of slab surface temperatures in the northeast corner zone over the course of a year. The series begins on October 17 and runs for 1 full year to the following October 16.

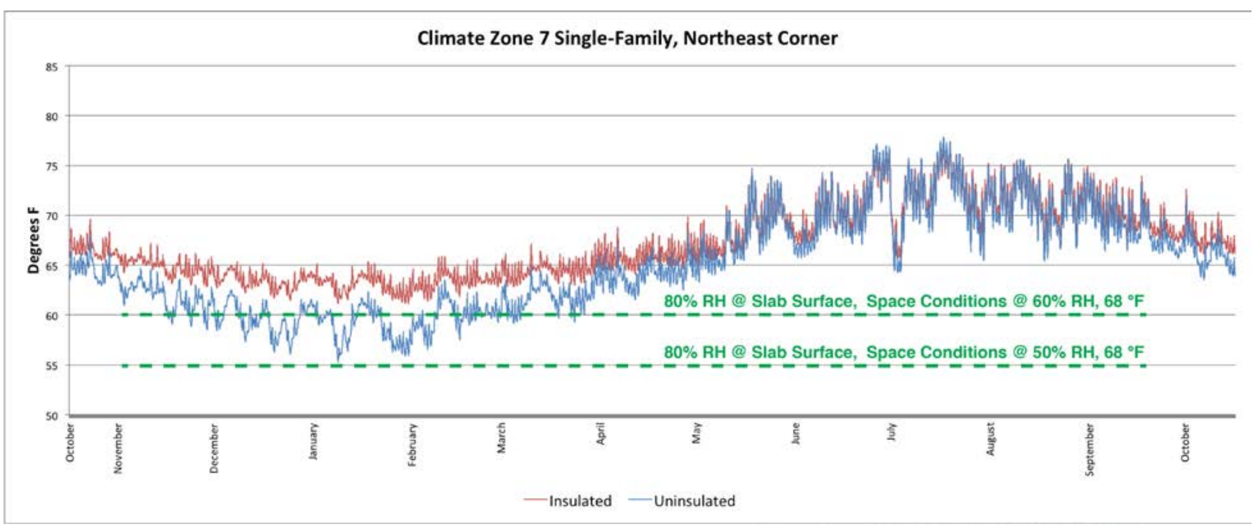

Figure 14. Zone 7 single-family slab corner temperatures

Per BEopt protocol, slabs in the simulation are covered with carpet, with an R-value of 1. In colder climates, the difference between the insulated and uninsulated cases becomes greater due to the larger difference between indoor and outdoor temperatures. In zone 7, winter slab surface temperatures on the uninsulated case dip as low as 55°F. In this case, indoor air at 68°F and 50% relative humidity (RH) would cause conditions at the slab surface to reach 80% RH, indicating a potential for mold growth.

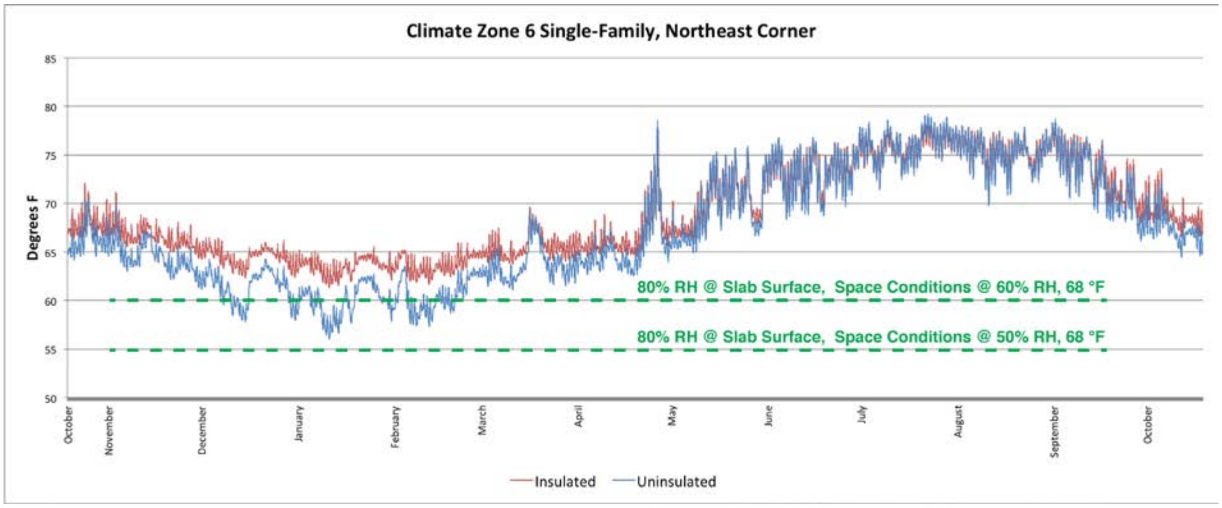

Figure 15. Zone 6 single-family slab corner temperatures

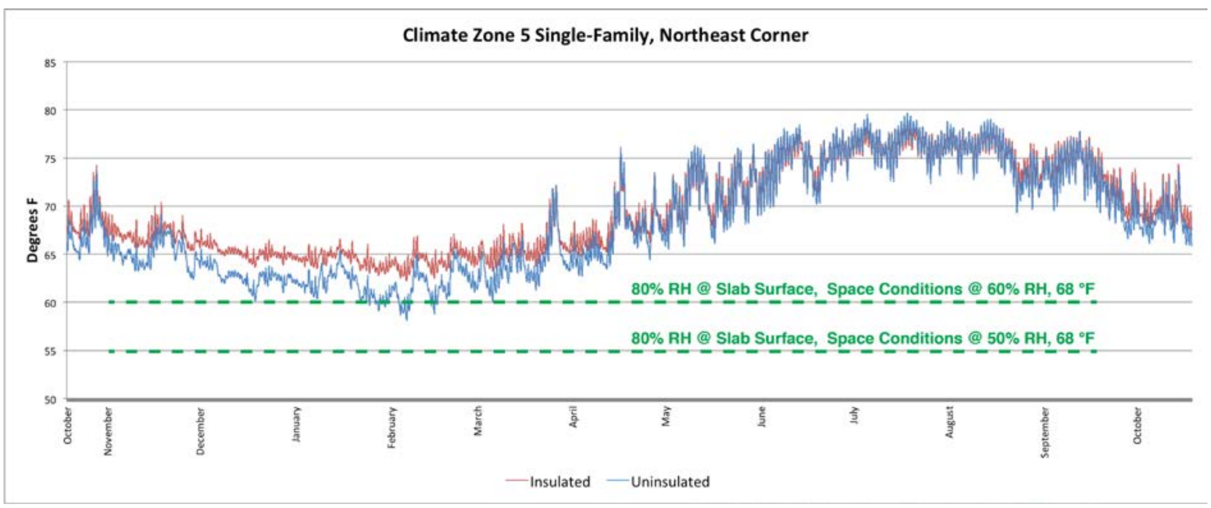

Figure 16. Zone 5 single-family slab corner temperatures

In zone 7, the insulated slab remains above approximately 62°F throughout the year (Figure 17) while the uninsulated slab temperature extends lower than 60°F during the heating season. This shift means that with SOG insulation, indoor conditions can drift to 60% RH before conditions at the slab reach 80%. This pattern repeats in zones 6 and 5, with maximum increased slab surface temperatures during peak cold weather of about 3°F. In zone 4, even the uninsulated case exceeds 60°F throughout the year.

The other nonenergy benefit is the floor temperature stabilizing at a value closer to the indoor ambient air temperature. This will improve thermal comfort as a consequence of decreasing the effect of radiant heat exchange with the slab surface in the indoor environment. In Zone 4 the phenomenon can be seen to operate even in the summer, when the slab surface remains cooler in the insulated case than the uninsulated case.

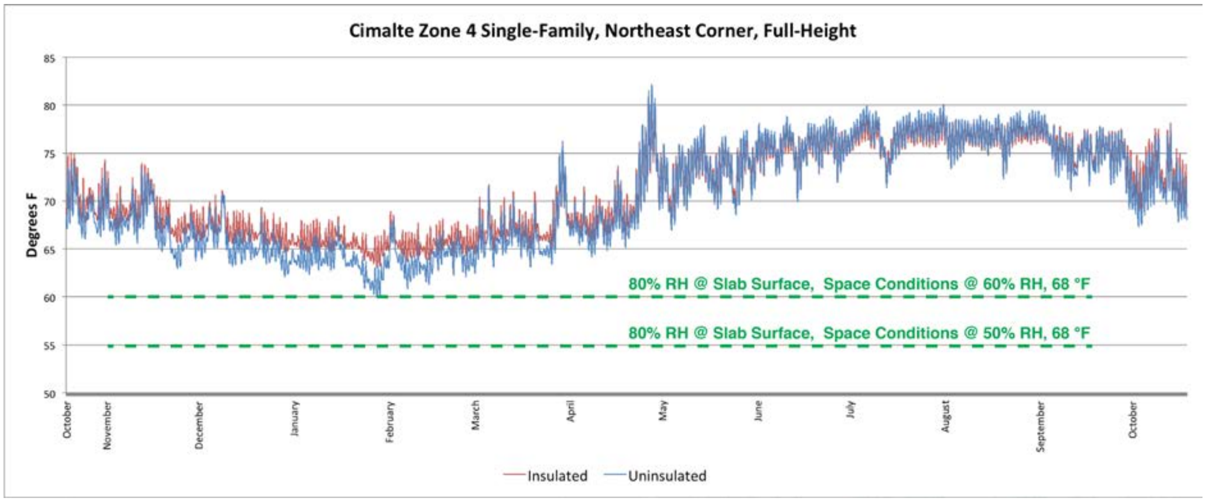

Figure 17. Zone 4 single-family slab corner temperatures

5.7 Analysis Summary

The simulation results for the four climate zones may be represented by the following approximation derived from the results given in Table 33 through Table 44 by multivariate analysis of the relationships between γ, β and σ:

$$(1 - \gamma_i) \approx \beta_u (1 - \sigma_i)$$

where:

γ_i = <insulated SOG foundation site energy>/<uninsulated SOG foundation site energy>

β_u = <uninsulated SOG slab heat flow>/<uninsulated SOG foundation site energy>

σ_i = <insulated SOG slab heat flow>/<uninsulated SOG slab heat flow>

Table 30 shows the approximate values of β_u required to achieve a 10% site energy savings for the four climate zones simulated by applying this relationship to the optimized SOG insulation system evaluated.

Table 30. Approximate Values of β_u for 10% Site Energy Savings

Building	Zones	Average Computed σ	Approximate βu
Single-Family	5–7	0.771	0.44
Single-Family	4	0.888	0.89
Multifamily	5–7	0.735	0.38
Multifamily	4	0.866	0.75

Table 30 suggests that 10% site energy savings from optimized SOG foundation insulation only becomes possible when the combined above-grade enclosure and occupant lifestyle energy consumption fraction of the site energy is reduced to 62% or less for zones 5–7, and, 25% or less for zone 4. Thus, to achieve high levels of cost-effective retrofit energy savings (>25%), SOG foundation insulation has a considerably lower priority than other measures in zones 5–7, and, it is likely never appropriate in zone 4 as achieving a β_u of 0.75 is exceedingly difficult in practice.

6 Answers to Research Questions

The answers to the research questions posed in Section 1.4 are provided below.

1. Can the experimentally measured site energy savings of a SOG foundation insulation in a cold climate be replicated by the BEB simulation model?

   A comparison of the simulation and experiment site energy savings yielded an error of 7 –3.2/+3.4%. Lower errors were not possible because of the difference between the experiment and simulation slab boundary conditions.

2. What is the energy performance and installation cost of a range of technically feasible SOG foundation insulation retrofit systems in climate zone 6?

   In Minneapolis, Minnesota, the site energy savings range from a maximum of 36% for the optimum insulation configuration to a minimum of 23% for 1-in. XPS full-wall insulation. 2012 IECC-compliant insulation yielded savings of 27.6%. The savings were simulated on a building with a <high slab heat flow/site energy>ratio (β) of 0.527 and cannot be realized on buildings with lower values of β. The maximum installation cost is $60.52/linear ft for half below-grade wall height vertical insulation together with 18 in. of wing insulation. The minimum cost of $14.68/linear ft is realized for half below-grade wall height vertical insulation with hydro-vacuum excavation. IECC 2012 insulation has an installation cost of $17.94/linear ft with hydro-vacuum excavation.

3. Can the experimentally measured site energy savings in zone 6 be met or exceeded in cold and intermediate climates by cost-effective SOG insulation strategies such as those developed for FPSFs?

   No. The experimentally measured site energy savings in zone 6 ranged from 13.1 to 14.3%. The maximum simulated site energy savings of 5% were realized for a single-family dwelling in Duluth.

4. What is the optimum SOG insulation retrofit strategy in zone 6 in terms of absolute energy savings and energy savings/retrofit cost/unit length of perimeter?

   Below grade: tapered insulation from grade (4 in. wide) to half the below-grade wall height (2 in. wide) consisting of 2 in. XPS with PPU foam between the XPS and the wall. Above grade: 4 in. of XPS insulation. Energy savings/retrofit cost/unit length of perimeter for a building with a <slab heat flow/site energy>ratio (β) of 0.527 are 14.5 Wh/$.ft.

5. What is the energy performance of the selected optimum SOG insulation retrofit strategy in four cities that span climate zones 4–7 for single- and multifamily homes?

   The zone 6 optimized insulation strategy was used for zones 5–7 and a unique strategy was used for zone 4. On this basis, for single-family homes, the site energy savings ranged from 3.1% in zone 4 to 5% in zone 7. Multifamily homes yielded site energy savings from 1.4% in zone 4 to 2.6% in zone 7. Time constraints did not permit the evaluation of climate-specific optimized SOG insulation retrofit strategies.

6. What is the installation cost of the optimum SOG insulation retrofit strategy in the four cities evaluated and the resultant cost-effectiveness of the retrofit measure?

See Table 31 and Table 32.

Table 31. Optimum SOG Insulation Cost-Effectiveness for Single-Family Home

Location	Zone	Cost for 180 Linear Feet ($)	Annual Total Energy Savings ($)	Simple Payback (year)
Duluth, MN	7	2993.90	66	45.4
Madison, WI	6	2363.00	52	45.4
Cleveland, OH	5	2055.65	44	47.1
Richmond, VA	4	1209.90	41	17.9

Table 32. Optimum SOG Insulation Cost-Effectiveness for Multifamily Home

Location	Zone	Cost for 250 Linear Feet ($)	Annual Total Energy Savings ($)	Simple Payback (year)
Duluth, MN	7	4158.20	91	45.6
Madison, WI	6	3281.95	70	46.6
Cleveland, OH	5	2855.07	60	47.4
Richmond, VA	4	1680.41	55	18.5

7 Conclusions

Comparing simulation and experimental site energy savings, the BEB simulation program achieved a nominal accuracy of 7% for a single case in a zone 6 climate. The inability of the BEB simulation to model the experimental slab heat transfer physics can plausibly account for a portion of the error. A new experiment to measure the convective heat transfer through the SOG interior surface is necessary to better validate the site energy performance of whole buildings with SOG foundations.

Two parameters are critical for achieving significant site energy savings for SOG foundations:

- The uninsulated slab heat flow fraction of the site energy consumption (β_u)
- The insulated slab/uninsulated slab heat flow ratio (σ_i).

For site energy savings of 10% or greater to be achieved in real-world houses, as an approximate guide, $\sigma_i \leq 0.7$, and $\beta_u \geq 0.38$ and 0.75 need to be achieved for single- and multifamily homes, respectively.

The optimized retrofit SOG foundation insulation that was developed consists of R-20 insulation at and above grade, tapering to R-10 at half the below-grade wall height. When applied to an idealized test building in zone 6 with β_u=0.53, this yielded a reduction in slab heat flow of 58% and a site energy savings of 36%.

Optimally insulated SOG foundations on real-world single-family homes yielded slab heat flow reductions ranging from 17% in Richmond (zone 4) to 31% in Duluth (zone 7). These reductions produced site energy savings of 3.7% and 5% (source energy savings of 2.4% and 3.9%) and simple paybacks of 17.9 and 45.4 years in Richmond and Duluth respectively.

Optimally insulated SOG foundations on real-world multifamily homes yielded slab heat flow reductions ranging from 15% in Richmond (zone 4) to 28% in Duluth (zone 7). These reductions produced site energy savings of 1.7% and 2.6% (source energy savings of 1% and 1.8%) and simple paybacks of 18.5 and 45.6 years in Richmond and Duluth, respectively.

SOG foundation insulation on single-family homes increased the cooling load in zones 6 and 7 but decreased the cooling load in zones 4 and 5. For multifamily homes, SOG insulation increased the cooling load in zones 5–7 and decreased the cooling load in zone 4 only.

In single-family homes, SOG foundation insulation increased the minimum slab surface temperature by about 3°F in zones 5–7 and by about 0.5°F or more in zone 4.

References

Adjali, M.H., Davies, M., and Littler, J. 1998. "Three-Dimensional Earth-Contact Heat Flows: A Comparison of Simulated and Measured Data for a Buried Structure." *Renewable Energy*, 15: 356–359.

Adjali, M.H., Davies, M., Rees, S.W., and Littler, J. 2000. "Temperatures in and under a Slab-on-Ground Floor: Two- and Three-Dimensional Numerical Simulations and Comparison with Experimental Data," *Building and Environment,* 35(7): 655–662.

Bejan A., and Lorente, S. 2004. "The Constructal Law and the Thermodynamics of Flow Systems with Configuration." *International Journal of Heat and Mass Transfer* 47: 3203–3214.

Chuangchid, P., and Krarti, M. 2001. "Foundation Heat Loss from Heated Concrete Slab-on-Grade Floors." *Building and Environment* 36(5): 637–655.

Dow. 2014. History of Dow Building Solutions. Dow Building Solutions, accessed November 4, 2014: http://building.dow.com/about/history.htm.

EIA. 2009a. 2009 Residential Energy Consumption Survey Data. U.S. Energy Information Administration, accessed October 30, 2014: www.eia.gov/consumption/residential/data/2009/.

EIA. 2009b. 2009 Table HC2.6 Structural and Geographic Characteristics of U.S. Homes, by Climate Region. U.S. Energy Information Administration, accessed October 30, 2014: www.eia.gov/consumption/residential/data/2009/xls/HC2.6%20Structural%20and%20Geographic%20by%20Climate%20Region.xls.

EIA. 2009c. 2009 Table HC2.3 Structural and Geographic Characteristics of U.S. Homes, by Year of Construction. U.S. Energy Information Administration, accessed October 30, 2014: www.eia.gov/consumption/residential/data/2009/xls/HC2.3%20Structural%20and%20Geographic%20by%20Year%20of%20Construction.xls.

EIA. 2014a. Electric Power Monthly with Data for August 2014. October 2014. U.S. Energy Information Administration: www.eia.gov/electricity/monthly/current_year/october2014.pdf.

EIA. 2014b. Natural Gas Annual, 2013. U.S. Energy Information Administration: www.eia.gov/naturalgas/annual/pdf/nga13.pdf.

Emery, A.F., Heerwagen, D.R., Kippenhan C.J., and Steele, D.E. 2007. "Measured and Predicted Thermal Performance of a Residential Basement." *HVAC&R Research*, 13(1): 39–57.

Goldberg, L.F., and Harmon, A.C. 2015. *Foundation Retrofit Experimental Hygrothermal Performance: Cloquet Residential Research Facility Laboratory Results* (Subcontractor Report). Golden, CO: National Renewable Energy Laboratory, NREL/SR-5500-63319. www.nrel.gov/docs/fy15osti/63319.pdf.

Goldberg, L.F., and Steigauf B. 2013. *Cold Climate Foundation Retrofit Energy Savings: The Simulated Energy and Experimental Hygrothermal Performance of Cold Climate Foundation*

Wall Insulation Retrofit Measures–Phase I, Energy Simulation (Subcontractor Report). Golden, CO: National Renewable Energy Laboratory, NREL/SR-5500-57333. www.nrel.gov/docs/fy13osti/57333.pdf .

Goldberg, L.F., Langenfeld, D.T. and Lively, R.L. 1994. Foundation Test Facility Experimental Results Part I: 1993/94 Test Period System Data, Underground Space Center research report, University of Minnesota.

Harmon, A.C. (2014). Master's Thesis, Department of Bioproducts and Biosystems Engineering, University of Minnesota, in preparation.

HUD. 1994. Design Guide for Frost-Protected Shallow Foundations, U.S. Department of Housing and Urban Development: www.huduser.org/Publications/PDF/FPSFguide.pdf.

HUD and Commerce. 2013. American Housing Survey for the United States: 2011, U.S. Department of Housing and Urban Development and U.S. Department of Commerce: www.census.gov/content/dam/Census/programs-surveys/ahs/data/2011/h150-11.pdf.

Huelman, P., Goldberg L., and Jacobson, R. 2015. *Innovative Retrofit Insulation Strategies for Concrete Masonry Foundations* (Subcontractor Report). Golden, CO: National Renewable Energy Laboratory, NREL/SR-5500-63139. www.nrel.gov/docs/fy15osti/63139.pdf.

Johansen, O. (1975). *Thermal Conductivity of Soils*. Ph.D. thesis. Trondheim, Norway (CRREL Draft Translation 637, 1977) ADA 044002.

Khaled, N., Rouissi K., and Krarti, M. 2012. "Impact of Layered Soil on Foundation Heat Transfer for Slab-on Grade Floors." *Journal of Solar Energy Engineering* 134(2): 021007 (8 pp.).

Labs, K., Carmody, J., Sterling, R.L., Shen, L., Huang, Y.J., and Parker, D. 1988. *Building Foundation Design Handbook*. University of Minnesota.

MN DLI (2012). Effective Dates of Minnesota Code and Rule Adoptions. Minnesota Department of Labor and Industry: www.dli.mn.gov/CCLD/PDF/sbc_dates.pdf.

Neymark, J., and Judkoff, R. (2008). *International Energy Agency Building Energy Simulation Test and Diagnostic Method (IEA BESTEST), In-Depth Diagnostic Cases for Ground Coupled Heat Transfer Related to Slab-On-Grade Construction* (Technical Report). Golden, CO: National Renewable Energy Laboratory, NREL/TP-550-43388.

Schirber, T., Mosiman, G., and Ojczyk, C. 2014. *Excavationless Exterior Foundation Insulation Field Study* (Subcontractor Report). Golden, CO: National Renewable Energy Laboratory, NREL/SR-5500-62556. www.nrel.gov/docs/fy15osti/62556.pdf.

Slattery, J.C. 1981. *Momentum, Energy and Mass Transfer in Continua*. Krieger, New York.

Tabares-Velasco, P.C. 2013. "Time Step Considerations When Simulating Dynamic Behavior of High-Performance Homes." *Proceedings Thermal Performance of the Exterior Envelopes of Whole Buildings XII*, paper no. 149, ASHRAE.

Appendix A: Slab-on-Grade Insulation Optimization Simulation Results

Table 33 reports the sum of the slab quadrant surface heat flows simulated by BUFETS and reported by EnergyPlus over the entire calendar year. The ratio of the BUFETS and EnergyPlus heat flow sums are compared. These data confirm that the data transfer mechanism between BUFETS and EnergyPlus is operating correctly; that is, in aggregate the slab surface heat flux data output by BUFETS are in agreement with the data input to EnergyPlus.

Table 34 shows the EnergyPlus results for the entire slab together with the simulated energy consumption, calculated values of σ, β, and γ, and the site energy savings.

Table 33. Full-Year BUFETS-B/EnergyPlus Heat Flow Consistency Check

Run Index	Insulation System Description	BUFETS Slab Quadrant Heat Flow (kWh)			Eplus Slab Quadrant Heat Flow (kWh)			Eplus/BUFETS Slab Quadrant Heat Flow Ratios		
		Center	Edge	Corner	Center	Edge	Corner	Center	Edge	Corner
R	Reference, no insulation, with windows	140.467	305.535	167.279	140.467	305.536	167.279	1.000	1.000	1.000
1	Insulation: 1-in. XPS, full wall	113.852	163.177	91.732	113.854	163.178	91.734	1.000	1.000	1.000
2	Insulation: 2-in. XPS, full wall	107.239	137.613	77.210	107.242	137.613	77.211	1.000	1.000	1.000
3	Insulation: 1-in. XPS, 1-in. PPU, full wall	106.875	135.714	76.079	106.927	135.733	76.087	1.000	1.000	1.000
4	Insulation: 2-in. XPS, 1-in. PPU, full wall	102.933	124.045	69.304	102.933	124.049	69.306	1.000	1.000	1.000
5	Insulation: 1-in. XPS, 2-in. PPU, full wall BG, tapered; 3-in. XPS AG	101.856	124.316	69.470	101.859	124.318	69.470	1.000	1.000	1.000
6	Insulation: 1-in. XPS, 2.5-in. PPU 3/4 wall BG, tapered; 3.5-in. XPS AG	101.271	123.003	68.558	101.273	123.003	68.558	1.000	1.000	1.000
7	Insulation: 2-in. XPS, 2-in. PPU, half wall BG, tapered; 4-in. XPS AG	102.432	128.141	71.286	102.433	128.142	71.286	1.000	1.000	1.000
8	Insulation: 2-in. XPS, 1-in. PPU, AG + half BG wall	106.720	135.274	75.371	106.721	135.274	75.370	1.000	1.000	1.000
9	Insulation: 2-in. XPS, 1-in. PPU, AG + half BG wall and interior floor	100.894	82.069	42.636	100.895	82.071	42.637	1.000	1.000	1.000
10	Insulation: 3-in. XPS, AG + half BG wall, 3-in. XPS 18-in. wide wing	102.089	127.274	71.073	102.089	127.275	71.075	1.000	1.000	1.000

Table 34. EnergyPlus Heating Season Results (10/13–5/5)

Run Index	Slab Heat Flow (kWh)				Electric Coil Energy (kWh)	Fan Energy (kWh)	Site Energy (kWh)	Slab Energy Fraction (β) (Slab/Site)	Slab Heat Flow Ratio (σ) (*/Base)	Site Energy Consumption Ratio (γ) (*/Base)	Site Energy Savings
	Center	Edge	Corner	Total							
R	–417.068	–1070.251	–595.665	–2,082.984	3,867.674	85.693	3,953.367	0.527	1.000	1.000	N/A
1	–307.444	–527.857	–306.396	–1,141.697	2,994.056	67.580	3,061.637	0.373	0.548	0.774	0.226
2	–280.309	–430.252	–250.854	–961.415	2,808.109	55.255	2,863.364	0.336	0.462	0.724	0.276
3	–278.617	–422.991	–246.534	–948.143	2,796.810	55.243	2,852.053	0.332	0.455	0.721	0.279
4	–262.752	–377.901	–220.318	–860.971	2,679.668	47.567	2,727.234	0.316	0.413	0.690	0.310
5	–258.357	–379.035	–221.000	–858.392	2,600.467	41.888	2,642.355	0.325	0.412	0.668	0.332
6	–255.857	–375.216	–218.123	–849.197	2,517.660	38.454	2,556.114	0.332	0.408	0.647	0.353
7	–259.740	–394.341	–228.188	–882.269	2,481.739	36.649	2,518.388	0.350	0.424	0.637	0.363
8	–277.420	–422.628	–244.378	–944.426	2,659.506	42.031	2,701.537	0.350	0.453	0.683	0.317
9	–255.272	–248.896	–134.261	–638.429	2,546.429	60.194	2,606.623	0.245	0.306	0.659	0.341
10	–257.261	–387.212	–225.292	–869.765	2,529.622	38.482	2,568.105	0.339	0.418	0.650	0.350

Appendix B: Single-Family Dwelling Slab-on-Grade Simulation Results

Table 35 reports the same data as Table 33 described in Appendix A.

Table 36 shows the data for the contiguous heating and cooling seasons only. The slab heat flow energy savings are highlighted in green. Increases in cooling energy consumption resultant from SOG insulation are highlighted in orange while decreases are highlighted in blue.

Table 37 reports the EnergyPlus results for a full calendar year. The slab heat flow ratio (σ) and site energy savings are highlighted in green.

Table 35. Full year BUFETS-B/EnergyPlus Heat Flow Consistency Check

Climate	Run Index	Configuration	BUFETS Quadrant Slab Abs. Heat Flow (kWh)			Eplus Quadrant Slab Abs. Heat Flow (kWh)			Eplus/BUFETS Slab Heat Flow Ratios		
			Center	Edge	Corner	Center	Edge	Corner	Center	Edge	Corner
Duluth, MN (Zone 7)	Z7-Ref	Reference	681.325	755.241	129.955	681.326	755.410	129.954	1.000	1.000	1.000
	Z7-Ins	OptInsul	596.612	404.241	73.382	596.613	404.311	73.383	1.000	1.000	1.000
Madison, WI (Zone 6)	Z6-Ref	Reference	511.164	618.170	106.876	511.165	618.311	106.876	1.000	1.000	1.000
	Z6-Ins	OptInsul	447.455	353.138	64.598	447.457	353.205	64.600	1.000	1.000	1.000
Cleveland, OH (Zone 5)	Z5-Ref	Reference	465.339	517.906	89.197	465.341	518.025	89.197	1.000	1.000	1.000
	Z5-Ins	OptInsul	416.616	306.091	55.542	416.617	306.148	55.539	1.000	1.000	1.000
Richmond, VA (Zone 4)	Z4-Ref	Reference	768.990	396.814	67.394	768.993	396.905	67.393	1.000	1.000	1.000
	Z4H-Ins	OptInsul-Half wall	718.033	293.100	51.530	718.035	293.161	51.530	1.000	1.000	1.000
	Z4F-Ins	OptInsul-Full wall	703.420	273.832	48.298	703.420	273.887	48.296	1.000	1.000	1.000

Table 36. EnergyPlus Contiguous Heating and Cooling Period Results

Run Index	Contiguous Heating Only Period						Contiguous Cooling Only Period			
	Dates	Slab Heat Flow (GJ)	Slab Heat Flow Ratio (σ) (*/Base)	Slab Heat Flow Savings	Heating Energy (GJ)	Slab Heat Flow Ratio (β) (Slab/Heating)	Dates	Slab Heat Flow (GJ)	Cooling Energy (GJ)	Effect of Insulation on Cooling Load (MJ)
Z7-Ref	09/18–5/16	–17.829	1.000	N/A	105.723	0.169	6/24–9/1	–2.787	0.505	
Z7-Ins	09/18–5/16	–10.686	0.599	0.401	97.421	0.110	6/24–9/1	–2.605	0.521	+16
Z6-Ref	10/1–5/5	–12.906	1.000	N/A	80.144	0.161	6/23–8/1	–2.149	2.009	
Z6-Ins	10/1–5/5	–7.964	0.617	0.383	74.472	0.107	6/23–8/1	–2.106	2.016	+7
Z5-Ref	9/28–5/4	–10.925	1.000	N/A	66.052	0.165	6/8–9/5	–2.524	2.593	
Z5-Ins	9/28–5/4	–6.941	0.635	0.365	61.563	0.113	6/8–9/5	–2.491	2.588	–5
Z4-Ref	9/30–4/30	–11.828	1.000	N/A	38.568	0.307	6/15–9/10	–3.055	3.777	
Z4H-Ins	10/1–4/30	–9.259	0.783	0.217	35.780	0.259	6/15–9/10	–3.234	3.722	–55
Z4F-Ins	10/1–4/30	–8.738	0.739	0.261	35.236	0.248	6/15–9/10	–3.252	3.717	–60

Table 37. Full-Year EnergyPlus Results

Run Index	Slab Heat Flow (GJ)					Heating Energy (GJ)	Eplus Cooling Energy (GJ)	HVAC Fan Energy (GJ)	Eplus Site Energy (GJ)	Slab Heat Flow Fraction (β) (Slab/Site)	Site Energy Consump. Ratio (γ) (*/Ref)	Site Energy Savings	Eplus Source Energy (GJ)	Source Energy Consump. Ratio (γ) (*/Base)	Source Energy Savings
	Center	Edge	Corner	Total	Slab Heat Flow Ratio (σ) (*/Ref)										
Z7-Ref	–9.81	–10.88	–1.87	–22.56	1.000	107.22	0.56	3.07	160.44	0.141	1.000	N/A	230.85	1.000	n/a
Z7-Ins	–8.59	–5.82	–1.06	–15.47	0.686	99.38	0.58	2.86	152.41	0.102	0.950	0.050	221.75	0.961	0.039
Z6-Ref	–7.36	–8.90	–1.54	–17.80	1.000	81.83	2.54	2.86	136.77	0.130	1.000	N/A	208.89	1.000	N/A
Z6-Ins	–6.44	–5.09	–0.93	–12.46	0.700	75.93	2.57	2.71	130.74	0.095	0.956	0.044	202.11	0.968	0.032
Z5-Ref	–6.70	–7.46	–1.28	–15.44	1.000	66.90	3.01	2.57	122.02	0.127	1.000	N/A	193.31	1.000	N/A
Z5-Ins	–6.00	–4.41	–0.80	–11.21	0.726	62.32	3.03	2.45	117.33	0.096	0.962	0.038	188.01	0.973	0.027
Z4-Ref	–11.07	–5.72	–0.97	–17.76	1.000	38.83	4.93	2.27	95.48	0.186	1.000	N/A	167.89	1.000	N/A
Z4H-Ins	–10.34	–4.22	–0.74	–15.30	0.862	36.03	4.88	2.19	92.56	0.165	0.969	0.031	164.44	0.979	0.021
Z4F-Ins	–10.13	–3.94	–0.70	–14.77	0.832	35.49	4.88	2.17	91.99	0.161	0.963	0.037	163.80	0.976	0.024

Appendix C: Multifamily Dwelling Slab-on-Grade Simulation Results

Table 38, Table 39, and Table 40 are for a center unit of the multifamily dwelling and correspond to Table 35, Table 36, and Table 37, respectively, that are described in Appendix B. Table 41 through Table 43 give the data for an end unit of the multifamily dwelling. Table 44 sums the results of Table 39 and Table 42 for the whole building while Table 45 sums the results of Table 40 and Table 43 for the whole building.

Table 38. Center Unit Full-Year BUFETS-B/EnergyPlus Heat Flow Consistency Check

Climate	Run Index	Configuration	BUFETS Quadrant Slab Abs. Heat Flow (kWh)			Eplus Quadrant Slab Abs. Heat Flow (kWh)			Eplus/BUFETS Slab Heat Flow Ratios		
			Center	Edge	Corner	Center	Edge	Corner	Center	Edge	Corner
Duluth, MN (Zone 7)	Z7C-Ref	Reference	327.318	211.466	N/A	327.317	211.466	N/A	1.000	1.000	N/A
	Z7C-Ins	OptInsul	303.930	111.900	N/A	303.931	111.901	N/A	1.000	1.000	N/A
Madison, WI (Zone 6)	Z6C-Ref	Reference	217.070	171.702	N/A	217.072	171.703	N/A	1.000	1.000	N/A
	Z6C-Ins	OptInsul	199.399	96.430	N/A	199.402	96.430	N/A	1.000	1.000	N/A
Cleveland, OH (Zone 5)	Z5C-Ref	Reference	206.707	146.491	N/A	206.708	146.491	N/A	1.000	1.000	N/A
	Z5C-Ins	OptInsul	191.139	84.688	N/A	191.141	84.688	N/A	1.000	1.000	N/A
Richmond, VA (Zone 4)	Z4C-Ref	Reference	361.356	114.088	N/A	361.358	114.087	N/A	1.000	1.000	N/A
	Z4CH-Ins	OptInsul-half wall	344.939	82.497	N/A	344.942	82.497	N/A	1.000	1.000	N/A
	Z4CF-Ins	OptInsul-full wall	340.355	76.710	N/A	340.356	76.710	N/A	1.000	1.000	N/A

Table 39. Center Unit EnergyPlus Contiguous Heating And Cooling Period Results

Run Index	Contiguous Heating Only Period						Contiguous Cooling Only Period			
	Dates	Slab Heat Flow (GJ)	Slab Heat Flow Ratio (σ) (*/Base)	Slab Heat Flow Savings	Heating Energy (GJ)	Slab Heat Flow Ratio (β) (Slab/Heating)	Dates	Slab Heat Flow (GJ)	Cooling Energy (GJ)	Effect of Insulation on Cooling Load (MJ)
Z7C-Ref	9/20–5/16	–5.418	1.000	N/A	41.254	0.131	6/23–9/4	–1.336	0.718	
Z7C-Ins	9/20–5/16	–3.815	0.704	0.296	39.382	0.097	6/23–9/4	–1.258	0.736	+18
Z6C-Ref	10/1–5/5	–3.711	1.000	N/A	29.567	0.125	5/26–9/3	–1.495	2.351	
Z6C-Ins	10/1–5/5	–2.501	0.674	0.326	28.188	0.089	5/26–9/3	–1.413	2.372	+21
Z5C-Ref	9/29–5/4	–3.274	1.000	N/A	23.194	0.141	5/24–9/28	–1.503	2.635	
Z5C-Ins	9/29–5/4	–2.267	0.692	0.308	22.098	0.103	5/23–9/28	–1.438	2.655	+20
Z4C-Ref	10/3–4/30	–4.256	1.000	N/A	10.195	0.417	5/6–10/2	–2.510	4.016	
Z4CH-Ins	10/3–4/30	–3.579	0.841	0.159	9.551	0.375	5/6–10/2	–2.503	4.015	–1
Z4CF-Ins	10/3–4/30	–3.441	0.809	0.191	9.426	0.365	5/6–10/2	–2.494	4.017	+2

Table 40. Center Unit Full-Year EnergyPlus Results

Run Index	Slab Heat Flow (GJ)					Heating Energy (GJ)	Eplus Cooling Energy (GJ)	HVAC Fan Energy (GJ)	Eplus Site Energy (GJ)	Slab Heat Flow Fraction (β) (Slab/Site)	Site Energy Consump. Ratio (γ) (*/Ref)	Site Energy Savings	Eplus Source Energy (GJ)	Source Energy Consump. Ratio (γ) (*/Base)	Source Energy Savings
	Center	Edge	Corner	Total	Slab Heat Flow Ratio (σ) (*/Ref)										
Z7C-Ref	–4.71	–3.05	N/A	–7.76	1.000	41.40	0.85	1.36	93.13	0.083	1.000	N/A	154.94	1.000	N/A
Z7C-Ins	–4.38	–1.61	N/A	–5.99	0.772	39.51	0.88	1.32	91.22	0.066	0.979	0.021	152.84	0.986	0.014
Z6C-Ref	–3.13	–2.47	N/A	–5.60	1.000	29.66	2.48	1.47	83.09	0.067	1.000	N/A	147.69	1.000	N/A
Z6C-Ins	–2.87	–1.39	N/A	–4.26	0.761	28.26	2.50	1.44	81.69	0.052	0.983	0.017	146.16	0.990	0.010
Z5C-Ref	–2.98	–2.11	N/A	–5.09	1.000	23.26	2.75	1.37	76.84	0.066	1.000	N/A	141.27	1.000	N/A
Z5C-Ins	–2.75	–1.22	N/A	–3.97	0.781	22.15	2.77	1.34	75.73	0.052	0.986	0.014	140.07	0.992	0.008
Z4C-Ref	–5.20	–1.64	N/A	–6.85	1.000	10.20	4.06	1.33	64.96	0.105	1.000	N/A	131.04	1.000	N/A
Z4CH-Ins	–4.97	–1.19	N/A	–6.16	0.899	9.56	4.06	1.32	64.29	0.096	0.990	0.010	130.29	0.994	0.006
Z4CF-Ins	–4.90	–1.10	N/A	–6.01	0.877	9.43	4.06	1.31	64.17	0.094	0.988	0.012	130.15	0.993	0.007

Table 41. End Unit Full-Year BUFETS-B/EnergyPlus Heat Flow Consistency Check

Climate	Run Index	Configuration	BUFETS Quadrant Slab Abs. Heat Flow (kWh)			Eplus Quadrant Slab Abs. Heat Flow (kWh)			Eplus/BUFETS Slab Heat Flow Ratios		
			Center	Edge	Corner	Center	Edge	Corner	Center	Edge	Corner
Duluth, MN (Zone 7)	Z7E-Ref	Reference	705.543	733.654	135.262	705.544	733.787	135.262	1.000	1.000	1.000
	Z7E-Ins	OptInsul	620.374	392.576	76.281	620.376	392.638	76.280	1.000	1.000	1.000
Madison, WI (Zone 6)	Z6E-Ref	Reference	518.155	598.391	110.842	518.157	598.503	110.842	1.000	1.000	1.000
	Z6E-Ins	OptInsul	454.905	341.415	66.882	454.909	341.471	66.883	1.000	1.000	1.000
Cleveland, OH (Zone 5)	Z5E-Ref	Reference	476.063	504.843	93.145	476.065	504.937	93.146	1.000	1.000	1.000
	Z5E-Ins	OptInsul	426.660	297.818	57.873	426.663	297.866	57.874	1.000	1.000	1.000
Richmond, VA (Zone 4)	Z4E-Ref	Reference	811.930	398.674	72.463	811.930	398.748	72.464	1.000	1.000	1.000
	Z4EH-Ins	OptInsul-half wall	758.849	294.187	55.288	758.850	294.238	55.288	1.000	1.000	1.000
	Z4EF-Ins	OptInsul-full wall	743.768	274.791	51.795	743.771	274.837	51.795	1.000	1.000	1.000

Table 42. End Unit EnergyPlus Contiguous Heating and Cooling Period Results

Run Index	Contiguous Heating Only Period						Contiguous Cooling Only Period			
	Dates	Slab Heat Flow (GJ)	Slab Heat Flow Ratio (σ) (*/Base)	Slab Heat Flow Savings	Heating Energy (GJ)	Slab Heat Flow Ratio (β) (Slab/Heating)	Dates	Slab Heat Flow (GJ)	Cooling Energy (GJ)	Effect of Insulation on Cooling Load (MJ)
Z7E-Ref	9/24–5/9	–8.225	1.000	N/A	71.642	0.115	6/24–9/2	–1.510	0.827	
Z7E-Ins	9/24–5/9	–5.091	0.619	0.381	68.021	0.075	6/23–9/2	–1.417	0.857	+30
Z6E-Ref	10/1–5/5	–6.362	1.000	N/A	54.266	0.117	6/15–9/9	–1.327	2.462	
Z6E-Ins	10/1–5/5	–3.963	0.623	0.377	51.525	0.077	6/15–9/9	–1.268	2.476	+14
Z5E-Ref	9/28–5/4	–5.454	1.000	N/A	43.598	0.125	6/3–9/5	–1.354	2.749	
Z5E-Ins	9/28–5/4	–3.504	0.643	0.357	41.436	0.085	6/3–9/5	–1.318	2.753	+4
Z4E-Ref	10/1–4/30	–6.280	1.000	N/A	22.513	0.279	6/15–9/29	–1.798	4.185	
Z4EH-Ins	10/1–4/30	–4.997	0.796	0.204	21.211	0.236	6/15–9/29	–1.858	4.166	–19
Z4EF-Ins	10/1–4/30	–4.735	0.754	0.246	20.956	0.226	6/15–9/29	–1.862	4.165	–20

Table 43. End Unit Full-Year EnergyPlus Results

Run Index	Slab Heat Flow (GJ)					Heating Energy (GJ)	Eplus Cooling Energy (GJ)	HVAC Fan Energy (GJ)	Eplus Site Energy (GJ)	Slab Heat Flow Fraction (β) (Slab/Site)	Site Energy Consump. Ratio (γ) (*/Ref)	Site Energy Savings	Eplus Source Energy (GJ)	Source Energy Consump. Ratio (γ) (*/Base)	Source Energy Savings
	Center	Edge	Corner	Total	Heat Flow Ratio (σ)										
Z7E-Ref	–5.08	–5.28	–0.97	–11.34	1.000	73.11	1.00	2.27	125.94	0.090	1.000	N/A	192.71	1.000	N/A
Z7E-Ins	–4.47	–2.83	–0.55	–7.84	0.692	69.34	1.03	2.17	122.10	0.064	0.970	0.030	188.43	0.978	0.022
Z6E-Ref	–3.73	–4.31	–0.80	–8.84	1.000	54.93	2.96	2.26	109.67	0.081	1.000	N/A	179.16	1.000	N/A
Z6E-Ins	–3.28	–2.46	–0.48	–6.22	0.703	52.11	2.99	2.20	106.80	0.058	0.974	0.026	175.97	0.982	0.018
Z5E-Ref	–3.43	–3.64	–0.67	–7.73	1.000	43.92	3.27	2.04	98.74	0.078	1.000	N/A	167.52	1.000	N/A
Z5E-Ins	–3.07	–2.14	–0.42	–5.63	0.728	41.73	3.29	1.99	96.51	0.058	0.977	0.023	165.03	0.985	0.015
Z4E-Ref	–5.85	–2.87	–0.52	–9.24	1.000	22.59	5.15	1.92	79.07	0.117	1.000	N/A	149.83	1.000	N/A
Z4EH-Ins	–5.46	–2.12	–0.40	–7.98	0.864	21.28	5.13	1.89	77.70	0.103	0.983	0.017	148.24	0.989	0.011
Z4EF-Ins	–5.36	–1.98	–0.37	–7.71	0.834	21.02	5.14	1.88	77.44	0.100	0.979	0.021	147.95	0.987	0.013

Table 44. Full Multifamily Dwelling EnergyPlus Contiguous Heating and Cooling Period Results (2 center + 2 end units)

Run Index	Contiguous Heating Only Period					Contiguous Cooling Only Period		
	Slab Heat Flow (GJ)	Slab Heat Flow Ratio (σ) (*/Base)	Slab Heat Flow Savings	Heating Energy (GJ)	Slab Heat Flow Ratio (β) (Slab/Heating)	Slab Heat Flow (GJ)	Cooling Energy (GJ)	Effect of Insulation on Cooling Load (MJ)
Z7-Ref	–27.286	1.000	N/A	225.791	0.121	–5.693	3.090	
Z7-Ins	–17.811	0.653	0.347	214.806	0.083	–5.350	3.188	+98
Z6-Ref	–20.146	1.000	N/A	167.667	0.120	–5.643	9.627	
Z6-Ins	–12.927	0.642	0.358	159.426	0.081	–5.361	9.697	+70
Z5-Ref	–17.457	1.000	N/A	133.584	0.131	–5.714	10.767	
Z5-Ins	–11.543	0.661	0.339	127.068	0.091	–5.512	10.816	+49
Z4-Ref	–21.072	1.000	N/A	65.416	0.322	–8.617	16.400	
Z4H-Ins	–17.151	0.814	0.186	61.523	0.279	–8.722	16.362	–38
Z4F-Ins	–16.351	0.776	0.224	60.765	0.269	–8.712	16.364	–36

Table 45. Full Multifamily Dwelling Full-Year EnergyPlus Results (2 center + 2 end units)

Run Index	Slab Heat Flow (GJ)					Heating Energy (GJ)	Eplus Cooling Energy (GJ)	HVAC Fan Energy (GJ)	Eplus Site Energy (GJ)	Slab Heat Flow Fraction (β) (Slab/Site)	Site Energy Consump. Ratio (γ) (*/Ref)	Site Energy Savings	Eplus Source Energy (GJ)	Source Energy Consump. Ratio (γ) (*/Base)	Source Energy Savings
	Center	Edge	Corner	Total	Slab Heat Flow Ratio (σ) (*/Ref)										
Z7-Ref	–19.59	–16.66	–1.95	–38.19	1.000	229.03	3.70	7.26	438.14	0.087	1.000	N/A	695.30	1.000	N/A
Z7-Ins	–17.69	–8.88	–1.10	–27.66	0.724	217.70	3.82	6.98	426.64	0.065	0.974	0.026	682.54	0.982	0.018
Z6-Ref	–13.71	–13.56	–1.60	–28.87	1.000	169.17	10.87	7.46	385.52	0.075	1.000	N/A	653.70	1.000	N/A
Z6-Ins	–12.29	–7.69	–0.96	–20.95	0.726	160.74	10.98	7.28	376.98	0.056	0.978	0.022	644.26	0.986	0.014
Z5-Ref	–12.81	–11.49	–1.34	–25.64	1.000	134.36	12.05	6.82	351.16	0.073	1.000	N/A	617.58	1.000	N/A
Z5-Ins	–11.65	–6.73	–0.83	–19.21	0.749	127.77	12.13	6.66	344.48	0.056	0.981	0.019	610.20	0.988	0.012
Z4-Ref	–22.10	–9.03	–1.04	–32.17	1.000	65.58	18.41	6.50	288.06	0.112	1.000	N/A	561.74	1.000	N/A
Z4H-Ins	–20.86	–6.61	–0.80	–28.27	0.879	61.67	18.38	6.42	283.98	0.100	0.986	0.014	557.06	0.992	0.008
Z4F-Ins	–20.51	–6.17	–0.75	–27.43	0.853	60.91	18.40	6.38	283.22	0.097	0.983	0.017	556.20	0.990	0.010

buildingamerica.gov

U.S. DEPARTMENT OF ENERGY | Energy Efficiency & Renewable Energy

DOE/GO-102015-4726 ▪ September 2015